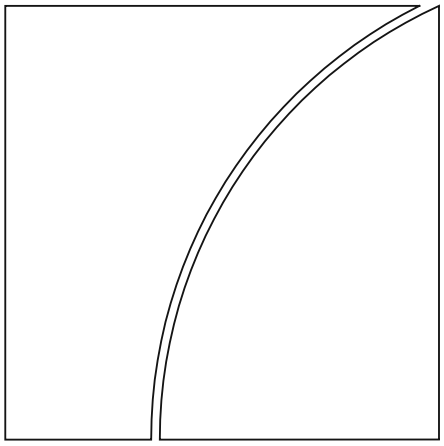

# BIS Working Papers

No 1361

## Bond yield responses to macro news: the role of macro forecast disagreement and monetary policy uncertainty

by Peter Hördahl, Burçin Kısacıkoğlu and Fan Dora Xia

Monetary and Economic Department

June 2026

JEL classification: E43, E44, G14

Keywords: macroeconomic news, forecast dispersion, policy uncertainty, bond yields, Bayesian learning

BIS Working Papers are written by members of the Monetary and Economic Department of the Bank for International Settlements, and from time to time by other economists, and are published by the Bank. The papers are on subjects of topical interest and are technical in character. The views expressed in this publication are those of the authors and do not necessarily reflect the views of the BIS or its member central banks.

This publication is available on the BIS website (www.bis.org).



ISSN 1020-0959 (print)
ISSN 1682-7678 (online)

# Bond Yield Responses to Macro News: The Role of Macro Forecast Disagreement and Monetary Policy Uncertainty

Peter Hördahl[1], Burçin Kısacıkoğlu[2] and Fan Dora Xia[3]

[1]*Bank for International Settlements**

[2]*Bilkent University and CEPR*†

[3]*Bank for International Settlements*‡

June 4, 2026

**Abstract**

Bond yields react to macroeconomic surprises, but the magnitude of this responsiveness depends on macroeconomic forecast disagreement and monetary policy uncertainty. Using intraday responses of US Treasury futures to surprises in macroeconomic data releases, we find that greater forecast disagreement about an economic indicator prior to its release dampens the yield curve response, while higher monetary policy uncertainty amplifies it. An exception is inflation surprises: prior to the post-COVID inflation surge, bond yield reactions to inflation surprises were not amplified by monetary policy uncertainty. We use a model with Bayesian learning to rationalize these findings. Specifically, large forecast disagreement indicates a weak link between the macroeconomic variable and future monetary policy, reducing the information value of macro news to forecast monetary policy. In contrast, during periods of high monetary policy uncertainty, macro news becomes more informative. Before the post-COVID inflation surge, investors may have perceived that the Federal Reserve placed little emphasis on its price stability mandate, which could have muted the yield curve response to inflation news even when policy rate uncertainty was high. The proposed model generates distinct, empirically testable effects of disagreement and monetary policy uncertainty on yield responses which, when extended to allow time-varying signal precision, accounts for the post-COVID shift in inflation sensitivity within a single unified framework.

***Keywords:*** Macroeconomic news, Forecast dispersion, Policy uncertainty, Bond yields, Bayesian learning

***JEL codes:*** E43; E44; G14

*Principal Economist. Email: Peter.Hoerdahl@bis.org.

†Assistant Professor of Economics and CEPR Research Affiliate. Email: bkisacikoglu@bilkent.edu.tr.

‡Principal Economist. Email: Dora.Xia@bis.org.

We thank Benjamin Born, Refet Gurkaynak, Giovanni Ricco, Andreas Schrimpf, Nikola Tarashev, CEPR MEF Annual Symposium, and BIS seminar participants for comments and suggestions. The views expressed herein are those of the authors, and do not necessarily reflect those of the Bank for International Settlements.

# 1 Introduction

It is well documented that the release of major macroeconomic indicators often leads to substantial re-pricing of bond yields in the US. For instance, Fleming and Remolona (1997) documented that 22 out of the 25 largest price movements in their sample period (1993–1994) were attributed to data releases, with the remaining driven by monetary policy announcements. Macroeconomic data releases are a primary source of public information about key macroeconomic variables, which in turn influence the expected path of monetary policy. Because these announcements are released simultaneously to all participants, the surprise, i.e. the deviation of the release from the publicly available consensus forecast, constitutes a common public signal that shifts all investors' beliefs at the same moment. As a result, when macroeconomic news is released, investors update their expectations for inflation and growth, revising the anticipated trajectory of policy rates and, consequently, the entire yield curve.

The pass-through from macroeconomic news to bond yield reactions, however, is state-contingent. Beber and Brandt (2010) find that bad news during economic expansions often triggers a larger response. Goldberg and Grisse (2013) show that bond yields typically increase in response to good news, but the magnitude of the reaction diminishes when risk levels are elevated. Swanson and Williams (2014) document that yield responses to macroeconomic news are dampened when monetary policy is constrained by the zero-lower bound or operating at ultra-low rates, anticipating the broader state-dependence framework we extend here, in which the conditioning state is forecast disagreement and short-rate uncertainty.

In this paper, we study how macroeconomic forecast disagreement and monetary policy uncertainty influence the pass-through of macro news. Both disagreement and uncertainty can affect the transmission of macroeconomic data surprises to bond yields by altering the informational value of these surprises to investors when revising their expectations of future monetary policy.

Empirically, we analyze intraday changes in bond yields in response to the release of six key macroeconomic variables: CPI, nonfarm payrolls, initial jobless claims, durable goods orders, retail sales, and GDP. To measure macroeconomic forecast disagreement, we use the cross-sectional standard deviation of survey forecasts collected by Bloomberg. For monetary policy uncertainty, we rely on the measure constructed by Bauer, Lakdawala, and Mueller (2022), which is derived from derivatives prices.

We find contrasting effects of disagreement and uncertainty: higher forecast disagreement dampens the reaction of bond yields, while greater monetary policy uncertainty amplifies it. This

pattern holds for most economic indicators in the pre-2020 sample, with one exception: bond yield reactions to inflation surprises were not amplified by short-rate uncertainty before the post-COVID inflation surge. The post-COVID period reveals two further departures from the pre-2020 pattern, in opposite directions. The CPI surprise response becomes positively conditional on short-rate uncertainty for the first time in our sample, while the nonfarm-payroll response, which had been strongly conditional on short-rate uncertainty pre-2020, weakens by roughly half and ceases to be statistically distinguishable from an unconditional reaction.

We then propose Bayesian learning models to interpret these results. In the baseline model, agents use macroeconomic announcements to forecast future short-term interest rates, which subsequently determine long-term bond yields. A large dispersion in expectations suggests a larger noise to signal ratio, i.e., a weaker relationship between the macroeconomic variable and future monetary policy, diminishing the informational value of macroeconomic news for forecasting monetary policy. Conversely, when uncertainty surrounding monetary policy is high, macroeconomic announcements are more informative about the path of future interest rates than when uncertainty is low. As a result, bond yields respond more strongly to macroeconomic announcements that coincide with lower forecast dispersion and greater monetary policy uncertainty. We further extend the model to allow for time-varying precision of macroeconomic announcements, which lets a single mechanism rationalize both post-COVID departures from the baseline pattern. CPI precision rises post-COVID as the Fed places more weight on inflation in its policy reaction function, amplifying the bond-market response to CPI surprises when policy uncertainty is high. Nonfarm payrolls (NFP) precision falls post-COVID, reflecting both deterioration in the BLS Current Employment Statistics survey (response-rate decline and historically large annual benchmark revisions) and structural dislocations in the labor market that make payroll prints noisier signals about the rate path.

A possible alternative interpretation of the dampening effect of disagreement involves a trading-channel story: when beliefs of investors are more heterogeneous, they are more willing to take the opposite side of a trade following a surprise, attenuating the price impact (e.g. Kandel and Pearson (1995)). We prefer our information-channel interpretation for two reasons. First, the trading channel does not jointly rationalize why short-rate uncertainty *amplifies* yield responses in the same data: greater uncertainty about the interest rate path would instead reduce optimal directional positions (Merton (1969)). Our model generates both effects, dampening from disagreement and amplification from short rate uncertainty, within a single Bayesian-learning mechanism. Second,

our interpretation generates a specific cross-sectional prediction, namely that disagreement should dampen responses more for releases with high diagnostic content (in line with our CPI/NFP subsample findings), which the trading channel would not predict.

Our modeling approach differs from the rational inattention framework of Sims (2003) and Maćkowiak and Wiederholt (2009), in which agents face a finite information-processing capacity and optimally choose what to attend to. In rational inattention models, signal precision is endogenous: agents who face greater uncertainty about a payoff-relevant variable allocate more capacity to tracking it, which endogenously reduces forecast disagreement. Disagreement and uncertainty are therefore jointly determined by the same capacity constraint. In our model, by contrast, disagreement arises from heterogeneity in forecasting models across agents, not from capacity limitations, and signal precision is exogenous to uncertainty. This separation allows disagreement and monetary policy uncertainty to operate as independent conditioning variables with distinct effects on yield responses, an empirical pattern that would be difficult to generate under rational inattention, where the two are tied together through the attention allocation decision. Our framework is closer in spirit to the imperfect-information tradition of Woodford (2003) and Mankiw, Reis, and Wolfers (2004), in which agents receive heterogeneous signals without optimizing over information acquisition.

The distinction matters empirically. Kroner (2025) documents a sharp increase in intraday market reactions to CPI releases during the 2021–2023 inflation surge, while reactions to other macro announcements remained largely unchanged. He attributes this selective increase to endogenous attention reallocation: investors shifted their information-processing capacity toward CPI, as measured by Bloomberg Terminal coverage in the days before each release. These findings are consistent with the modeling framework proposed by Pfäuti (2026), where inflation expectations feature state-dependent attention levels. Specifically, in this framework, agents pay more attention to inflation when it exceeds an attention threshold, and expectations become more sensitive to inflation. Our post-COVID results are consistent with Kroner's finding of heightened CPI sensitivity, but we offer a different mechanism. In our extended model, the increased CPI responsiveness reflects an exogenous change in signal precision: the precision of CPI as a signal about future monetary policy increased in the post-COVID period, making inflation surprises more informative about future policy rates regardless of how much attention investors allocate. The same precision channel, applied symmetrically, explains the post-COVID weakening of the NFP response we document: the precision of payrolls as a signal about the rate path declined, both for measurement

reasons (response-rate-driven noise in the establishment survey, larger revisions, structural shifts) and because CPI displaced payrolls as the marginal signal of policy direction. The two explanations are complementary: Kroner identifies *who* is paying more attention, while our framework explains *why* the signal became worth attending to (and, in the case of payrolls, why the signal lost diagnostic value).

Our paper is closely related to the literature on how disagreement and uncertainty influence the re-pricing of financial assets in response to surprises in macroeconomic announcements. Consistent with our findings, Born, Dovern, and Enders (2023) show that the sensitivity of equity prices to macroeconomic news decreases with greater expectations disagreement; and Pericoli and Veronese (2015) find that long-term yields and the exchange rate react less to macroeconomic surprises when forecaster heterogeneity is more pronounced. However, Born, Dovern, and Enders (2023) also find that the reaction weakens when monetary policy uncertainty is high. This divergence may reflect the different relationships that bonds and equities have with monetary policy.

The paper also contributes to the literature on the reaction of financial assets to macroeconomic news. Among many others, Balduzzi, Elton, and Green (2001), Boyd, Hu, and Jagannathan (2005), Gürkaynak, Sack, and Swanson (2005), Andersen et al. (2007) and Faust et al. (2007) document that macroeconomic news substantially affects bond yields, equity prices, and exchange rates, respectively.Altavilla, Giannone, and Modugno (2017) document that these announcement-driven adjustments are persistent. Hirshleifer and Sheng (2022) find that macroeconomic announcements lead to stronger response of equity returns to firm-level earnings announcements. The high-frequency event-study methodology we employ builds on the seminal work of Kuttner (2001) and Bernanke and Kuttner (2005) on monetary policy surprises, Nakamura and Steinsson (2018) on the information effects of policy announcements, and Gürkaynak, Kısacıkoğlu, and Wright (2020) on identifying news effects when announcement surprises are only partially measured by the consensus forecast — a measurement issue that maps directly into the structural-versus-measured-surprise distinction we formalize in Section 5.7.

Our work also relates to the literature on forecast disagreement and uncertainty. The interpretation of cross-sectional forecast dispersion as a measure of information heterogeneity draws on Mankiw, Reis, and Wolfers (2004), Patton and Timmermann (2010), and the information rigidity framework of Coibion and Gorodnichenko (2012) and Coibion and Gorodnichenko (2015). For monetary policy uncertainty, our measure follows Bauer, Lakdawala, and Mueller (2022), and our findings complement the broader literature on economic policy uncertainty (Baker, Bloom,

and Davis, 2016) and the identification of monetary shocks in bond and equity markets (Cieslak and Pang, 2021). Using these measures, Barbera, Xia, and Zhu (2023) show that higher levels of inflation forecasts disagreement and monetary policy uncertainty can dampen the transmission of monetary policy shocks to real economy.

The remainder of the paper is organized as follows: section 2 introduces our empirical framework; section 3 describes the dataset; section 4 shows the empirical results; section 5 presents a model to rationalize our empirical findings; section 6 performs a simulation exercise aimed at gauging the quantitative implications of the model; section 7 concludes.

## 2 Empirical Specification

The empirical specification follows the event study literature, in which intraday changes in yields are regressed on various macroeconomic surprises to identify the effects of news on the yield curve. However, we extend the standard event study regression by interacting macroeconomic surprises with release disagreement and short-rate uncertainty.

Following Born, Dovern, and Enders (2023), the regression equation has the form:

$$\Delta y_{n,t} = \alpha + \sum_{k=1}^{I} (\beta_{1,n}^k s_t^k + \beta_{2,n}^k \text{disp}_t^k + \beta_{3,n}^k (s_t^k \times \text{disp}_t^k)) + \beta_{4,n} \text{SRU}_t + \sum_{k=1}^{I} \beta_{5,n}^k (s_t^k \times \text{SRU}_t) + \beta_{6,n} X_t + \varepsilon_t \tag{1}$$

where $\Delta y_{n,t}$ is the 20-minute yield change (5 minutes before and 15 minutes after) of an $n$ period bond around a macroeconomic release, $s_t^k$ is a standardized surprise for the release $k$, $\text{disp}_t^k$ is the survey dispersion associated with the release $k$, $\text{SRU}_t$ is the short rate uncertainty[1], $X_t$ includes concurrent headline surprises in the same release considered in the regression, a zero lower bound dummy, as well as quadratic terms and other controls. Time subscript $t$ indexes the day of the macroeconomic announcement. The regression coefficients are maturity-specific, denoted with subscript $n$. We are interested in how the marginal impact of news on bond yields, particularly how it depends on short-rate uncertainty $\text{SRU}_t$ and survey dispersion (disagreement) $\text{disp}_t^k$.

Survey dispersion associated with a release $k$ at time $t$ is measured as the cross-sectional standard deviation of survey forecasts $f$:

$$\text{disp}_t^k = \sqrt{\frac{1}{J_{k,t}} \sum_{j=1}^{J_{k,t}} \left( f_{j,t}^k - \bar{f}_t^k \right)^2} \tag{2}$$

[1] Both disagreement and uncertainty measures are standardized by their respective standard deviations.

where $J_{k,t}$ is the number of survey participants for release $k$ at time $t$, $j = \{1, 2, \cdots, J_{k,t}\}$ is an index for individual forecasters, and $\bar{f}_t^k$ is the average of survey expectations as of time $t$, given by:

$$\bar{f}_t^k = \frac{1}{J_{k,t}} \sum_{j=1}^{J_{k,t}} f_{j,t}^k.$$

A couple of features of these survey data are worth noting for the information environment we have in mind. First, the individual forecasts $f_{j,t}^k$ are submitted before the announcement and reflect each forecaster's own private information about the upcoming release; the cross-sectional dispersion $\text{disp}_t^k$ therefore reflects private-signal heterogeneity across forecasters, as formalized in Section 5.2. Second, the consensus forecast $\bar{f}_t^k$ is itself publicly observable prior to the release and is the the publicly available baseline from which the announcement surprise is measured. The consensus thus plays the role of a public aggregation of private signals: it is informative about the true state of the economy but noisy when individual signals are more dispersed. The short-rate uncertainty $\text{SRU}_t$ is conceptually distinct from this dispersion: it captures uncertainty about the monetary policy regime, i.e. how the Fed will map a given macro state into the policy short rate, rather than noise in forecasters' private signals or in the announcement itself.

## 3 Data

We focus on intraday movements of 2-, 5-, and 10-year US Treasury futures in response to six 8:30 a.m. macroeconomic announcements: CPI, initial claims, nonfarm payrolls, durable goods, retail sales, and GDP. These releases are chosen because they elicit substantial yield curve responses (Gürkaynak, Kısacıkoğlu, and Wright, 2020). We use the 20-minute change in Treasury futures (5 minutes before and 15 minutes after) around these announcements as the outcome variable. Intraday US Treasury futures are from TickData and Reuters.

Macroeconomic surprises are defined as the difference between the release and the associated Bloomberg median forecast submitted by financial market participants. Given that the chosen releases have different units (for example, non-farm payrolls are in thousands and CPI is in percentages), we standardize the surprises to have the same units for ease of interpretation. Standardized surprise associated with release $k$ is calculated as:

$$s_t^k = \frac{a_t^k - f_t^k}{\sigma^k} \tag{3}$$

where $a_t^k$ is the actual announcement, $f_t^k$ is the median survey forecast, and $\sigma^k$ is the standard deviation of the raw surprise. Actual announcements and median forecasts are from Action Economics and Bloomberg. Survey dispersions are also demeaned and standardized with sample standard deviation, calculated using Bloomberg surveys.

The short rate uncertainty variable $\text{SRU}_t$ is the measure developed by Bauer, Lakdawala, and Mueller (2022). It is a daily measure derived from prices of Eurodollar futures and options. This measure has important advantages compared to other uncertainty measures. First, their measure is a high-frequency forward-looking measure derived from financial market prices. Although there are other measures of economic and monetary policy uncertainty, they are on a monthly frequency, which is less consistent with the empirical specification considered in this study. Second, while there are other high-frequency uncertainty measures, $\text{SRU}_t$ captures interest rate uncertainty better than these measures, as explained in detail in Bauer, Lakdawala, and Mueller (2022). They provide short rate uncertainty measures for 6-, 12-, 18-, and 24-month horizons, where we use the 12-month ahead uncertainty for the benchmark results. Given how the short rate uncertainty is measured, it would respond to macroeconomic surprises to the extent that these surprises affect monetary policy. The endogeneity between macroeconomic surprises and the $\text{SRU}_t$ requires the use of a one-day lag of the short rate uncertainty measure in the regression. Also, using a one day lagged short rate uncertainty is consistent with how survey dispersion is measured in the analysis. $\text{SRU}_t$ is demeaned and standardized with its sample standard deviation.

A similar endogeneity concern applies to survey disagreement: forecast dispersion is mechanically related to the difficulty of predicting a given release, which may itself correlate with surprise magnitude. Since disagreement is determined before the announcement window and reflects cross-sectional heterogeneity across forecasters rather than market prices, the concern is less acute than for $\text{SRU}_t$, but we cannot rule out that disagreement proxies for unobserved features of the macro environment that independently affect yield sensitivity.

Our identification relies on a high-frequency event-study assumption: within the 20-minute window centered on the release, the announcement surprise is the dominant news event, and any unobserved factors correlated with disagreement or short-rate uncertainty do not move yields differentially during this narrow window. Lagging $\text{SRU}_t$ by one day breaks within-day reverse causality but does not address persistence-driven correlation with macro regimes; we therefore include controls for VIX, MOVE, EPU, and the Jurado–Ludvigson–Ng macroeconomic uncertainty index in $X_t$, plus a zero-lower-bound dummy and quadratic terms in the conditioning variables,

so that the interaction coefficients $\beta_3^k$ and $\beta_5^k$ identify the marginal change in yield sensitivity to surprise $k$ holding fixed the level of broad financial-market and macro uncertainty. Under this conditioning, the coefficients we report should be read as state-contingent yield-sensitivity slopes rather than as the causal effects of disagreement or uncertainty in isolation.

We test this identifying assumption directly with a permutation-based placebo exercise reported in Section 4.4.

The sample is from June 1998 to September 2024, but we drop the period between March 2020 and June 2020 due to COVID-related complications in financial markets and extreme observations of macroeconomic surprises. Treasury market liquidity had been severely affected during the onset of the COVID-19 pandemic, especially between March and May 2020 (Logan (2020)). After the Fed's intervention in mid-March 2020, Treasury market liquidity recovered around May 2020. However, we still see extreme macroeconomic surprises until the end of May 2020, which can affect inference regarding how futures respond to surprises. To get a clearer picture, we remove this period from the analysis.[2]

# 4 Empirical Results

In this section, we present the regression results for two subsamples: the pre-2020 period (1998–February 2020) and the post-COVID period (July 2020–2024). We split the sample to examine how the yield curve response to macroeconomic surprises changed after the COVID-19 pandemic and the associated shifts in the Federal Reserve's policy framework. In particular, we are interested in the following partial derivative:

$$\frac{\partial \Delta y_{n,t}}{\partial s_t^k} = \beta_{1,n}^k + \beta_{3,n}^k \times \text{disp}_t^k + \beta_{5,n}^k \times \text{SRU}_t$$

where $\beta_{1,n}^k$ is the standard event study coefficient measuring the yield response of an $n$-period bond to the surprise $k$. $\beta_{3,n}^k$ measures how this response changes as the survey disagreement changes for a given level of short-rate uncertainty. Similarly, $\beta_{5,n}^k$ measures how the event study coefficient for surprise $k$ changes with the short rate uncertainty, keeping the survey dispersion

[2]We additionally drop five extreme NFP forecast-disagreement observations from April–August 2020, all with cross-sectional dispersion exceeding 500 (relative to typical pre-2020 values around 30), reflecting COVID-era forecaster confusion about payroll dynamics. Three of the five dates fall within the March–June 2020 gap that is already excluded from the regression samples; two (July 2 and August 7, 2020) are post-July 2020 dates that drop from the post-COVID sample. Including these observations would inflate the standard deviation of NFP forecast disagreement by roughly an order of magnitude, distorting the standardization of $\text{disp}_t^{\text{NFP}}$. An analogous COVID-era spike in initial-claims dispersion (March–May 2020) is contained within the already-excluded gap.

fixed. In the following, we plot the marginal effects of disagreement and short-rate uncertainty.The marginal effects are derived by assuming all variables at their means (which are zero) and varying the relevant right hand side variable (either the short rate uncertainty or survey dispersion) to estimate the effect on the event study coefficient.

### 4.1 Pre-2020 Results

The regression estimates for the pre-2020 sample are reported in Table 1, and the corresponding marginal effects for the two-, five-, and ten-year Treasury futures are given in Figure 1, Figure 2, and Figure 3, respectively. For most surprises considered, higher survey dispersion dampens the yield response, whereas higher short-rate uncertainty strengthens it. Note that the results for initial claim surprises are reversed. This reflects the counter-cyclical nature of the series: a positive surprise is associated with monetary policy easing, while for other indicators a positive surprise typically suggest tightening.

The pre-2020 results also reveal an interesting pattern for CPI surprises. Unlike the other macroeconomic indicators, the response of Treasury futures to CPI surprises is not sensitive to short rate uncertainty. Before the post-COVID inflation surge, CPI surprises apparently carried limited information about the future path of monetary policy even during periods of elevated policy uncertainty.

### 4.2 Post-COVID Results

The regression estimates for the post-COVID sample are reported in Table 2, and the corresponding marginal effects are given in Figure 4, Figure 5, and Figure 6, respectively. Comparing the post-COVID results to the pre-2020 results reveals two patterns worth noting. First, the dependence of the yield response to CPI surprises on short-rate uncertainty changes sign: the CPI $\times$ SRU interaction is essentially zero and insignificant in the pre-2020 sample, but becomes positive and highly significant post-COVID across all three maturities. This is the sign-flip that motivates our learning story. Second, the state-dependence of the nonfarm payrolls response on short rate uncertainty *weakens* across subsamples: the nonfarm payrolls (NFP) $\times$ SRU interaction is positive and significant in the pre-2020 sample at all maturities, but the point estimates contract by roughly half to two-thirds post-COVID and none remain statistically significant. The NFP $\times$ disagreement interaction declines even more sharply, from approximately $-0.2$ in the pre-2020 sample to near zero post-COVID, and likewise loses significance. The post-COVID changes in

CPI and NFP responses thus run in opposite directions: CPI becomes more state-dependent on short-rate uncertainty, while NFP becomes less so.

### 4.3 Interpreting the Subsample Differences

Before turning to the formal break tests, it is important to emphasize that the post-COVID amplification of the CPI surprise response is a theoretically motivated prediction rather than a finding selected ex post from a multiple-comparisons exercise. The mechanism we examine in Section 5.10 – a release-specific increase in CPI's diagnostic content for monetary policy following the 2021–2023 inflation surge – was anticipated by both the macro-finance and policy literatures. Bauer, Pflueger, and Sunderam (2025) document a shift in the market-perceived Federal Reserve reaction-function parameters around the inflation surge, with inflation receiving substantially larger implied weight in the post-2021 period. Kroner (2025) reports a sharp rise in intraday market reactions to CPI surprises during the inflation surge and attributes it to endogenous attention reallocation, with our extended Bayesian-learning model providing a complementary structural interpretation in terms of an increase in $\Delta\mu_t^{\text{cpi}}$. Xia and Zhu (2025) similarly documents a regime shift in how government bond yields respond to inflation news. The CPI sign-flip we examine below, the structural break test we now describe, and the SMM estimation in Section 6.4 should therefore be read as joint tests of a single ex-ante hypothesis, not as one striking finding pulled from a wider search.

The differences between the pre-2020 and post-COVID subsamples are not only economically meaningful but also statistically significant. Because our interpretation centers on the changing informativeness of inflation releases, we test for a structural break in the CPI-related coefficients specifically, restricting the sample to CPI-release dates so that the degrees of freedom in the test denominator reflect the actual CPI release observations rather than the pooled all release sample. The test examines three coefficients: the CPI surprise coefficient, its interaction with CPI release disagreement, and its interaction with short rate uncertainty. We interact a post-COVID indicator with those three regressors and $F$-test their joint significance; the $F$-test itself is direction agnostic, so we additionally report the point estimate of the pre-to-post shift in the SRU interaction coefficient ($\Delta\beta_{\text{SRU}}$), which directly gives the sign and magnitude of the change most relevant to the paper's mechanism.

Panel A of Table 3 reports the CPI result. The null of no break is rejected at conventional levels for all three maturities. The shift $\Delta\beta_{\text{SRU}}$ is positive and statistically significant, indicating that the

CPI $\times$ SRU interaction strengthened from the pre-2020 to the post-COVID subsample. This is the direction predicted by the learning model in Section 5: as CPI releases became more diagnostic about the policy path (higher $\Delta\mu/\sigma_a^2$ in the notation of that section), their interaction with short-rate uncertainty amplified.

Panel B reports the analogous subset test for the nonfarm payrolls coefficients on the NFP-release subsample. The null of no break is again rejected, but in contrast to Panel A, $\Delta\beta_{\text{SRU}}$ for NFP is negative, indicating that the NFP $\times$ SRU interaction *weakened* rather than strengthened post-COVID. This direction matches the subsample regression tables (Tables 1 and 2), in which the NFP $\times$ SRU coefficient is positive and significant pre-2020 at all maturities (0.0932, 0.0710, 0.0352) but contracts post-COVID (0.0166, 0.0244, 0.0208) and loses statistical significance; the NFP $\times$ disagreement interaction declines by a comparable proportion, from $(-0.176, -0.260, -0.220)$ pre-2020 to $(-0.034, -0.026, -0.016)$ post-COVID, and likewise loses significance. The Panel B result is thus consistent with payroll releases becoming less state-dependent, a decline rather than a rise in their diagnostic content for the near-term rate path. Panel C reports the full-coefficient Chow test on the pooled all-release sample as a joint diagnostic.

Why do the responses differ across subsamples? We argue that during the post-COVID inflation surge, CPI surprises became substantially more informative about the path of short-term interest rates. The surge in inflation that began in mid-2021 and persisted through 2023 brought consumer prices to the center of policy deliberations in a way not seen since the 1980s. As inflation rose well above the Fed's 2 percent target, CPI releases acquired outsized relevance for predicting the pace of rate hikes, and each print carried direct implications for the near-term policy path (Bauer, Pflueger, and Sunderam (2025) and Xia and Zhu (2025)). Kroner (2025) documents this shift directly: intraday market reactions to CPI surprises increased sharply during the inflation surge, while reactions to other macro releases remained largely unchanged, consistent with CPI becoming a more precise signal about future policy rates. In the language of the model below, the diagnosticity of the CPI release across policy regimes widened (or the predictive variance fell), raising the information content, and amplifying the yield response when short-rate uncertainty is elevated.

The nonfarm payrolls response tells a different story. Pre-2020, the NFP $\times$ SRU interaction was strongly positive and significant, consistent with payrolls being a key diagnostic signal for monetary policy when the rate path was uncertain. Post-COVID, this interaction weakens toward zero and loses statistical significance. Two not mutually exclusive interpretations are consistent with the

model. First, post-pandemic labor market data became unusually noisy. The response rate of the BLS Current Employment Statistics survey declined from roughly 60 percent before the pandemic to under 45 percent afterwards, raising measurement variance in preliminary payroll estimates (Leduc, Oliveira, and Paulson (2025)). Annual benchmark revisions through this period were also historically large: the August 2024 preliminary benchmark, published by the BLS, reduced the level of nonfarm payrolls by approximately 818,000 jobs for the twelve months ending March 2024 – the largest downward annual benchmark revision since 2009. Structural dislocations in the labor market itself (pandemic exits, sectoral reallocation, and large changes in labor force participation) add to the noise (Hobijn and Şahin (2023)). In the language of our model in Section 5 , these forces raise the predictive variance of payroll releases and therefore depress their diagnostic content. Second, once CPI became the dominant policy signal, payrolls carried less incremental information about the near-term rate path. Either way, payroll releases became a less state-dependent signal for bond markets post-COVID, consistent with the model's prediction that the yield response is amplified by SRU only when the release is diagnostic about the regime.

### 4.4 Permutation Placebo Tests

To test the identifying assumption directly, we conduct a permutation-based placebo exercise that re-estimates equation (1) repeatedly with randomly reshuffled surprise values. Within each release type $k$, the values of $s_t^k$ on the announcement dates are randomly permuted across dates while the yield changes $\Delta y_{n,t}$, disagreement $\text{disp}_t^k$, short-rate uncertainty $\text{SRU}_t$, and all controls in $X_t$ are held fixed; the full regression specification is then re-estimated, and the procedure is repeated 1,000 times to build a permutation null distribution for each interaction coefficient. Under the null that the interaction coefficients $\beta_3^k$ and $\beta_5^k$ in the announcement-window regressions are spurious products of persistent macro-regime correlations rather than effects of the actual realized surprise on each release date, permuted-surprise estimates should be centered at zero, and the actual estimates documented in Tables 1–2 should not be extreme relative to the permutation null. Table 6 reports the permutation null distribution and the corresponding two-sided permutation $p$-values across all six release types, three maturities, and two subsamples. The headline interaction coefficients documented in Tables 1–2 are extreme relative to the permutation null at conventional significance levels: the CPI $\times$ SRU interactions post-COVID have permutation $p$-values of 0.003, 0.000, and 0.001 at the 2-, 5-, and 10-year maturities respectively, and the NFP $\times$ disagreement and NFP $\times$ SRU interactions pre-2020 have permutation $p$-values below 0.02 at the 2- and 5-year

maturities for both interaction types. By contrast, the post-COVID NFP interaction coefficients are not extreme relative to the permutation null, a result consistent with the diminished diagnostic content of payroll releases documented in Sections 5.10 and 6.4. Across all seventy two interaction cells reported in Table 6, roughly twenty five percent have permutation $p$-values below 0.05 – well above the five percent rate that would obtain under the null of no real interaction effect – supporting the interpretation that the state-dependent yield sensitivity we measure reflects the actual realized surprise on each release date rather than spurious correlations between persistent regime variables and yield variability.

In the following section, we propose a model that can explain the changes in response and the importance of surprises during times of high short rate uncertainty.

# 5 Theoretical Model

We develop a two-day Bayesian learning model in which agents simultaneously learn about the state of the economy and about the monetary policy rule that maps the state into the short rate. The model produces two empirically testable predictions: the yield response to a macroeconomic surprise (i) falls with forecast disagreement and (ii) rises with short-rate uncertainty. We derive closed-form expressions for the event-study coefficient and characterize the conditions under which each prediction holds.

## 5.1 Environment and Timing

The economy lives for two days, $d-1$ (pre-announcement) and $d$ (announcement). Three primitives drive the model. The first is the latent macroeconomic state $x_d$ following a stationary AR(1) process. The second primitive is the latent policy regime $g_d \in \{H, L\}$ that jointly governs (i) the short-rate sensitivity to the state and (ii) the conditional mean of the announcement — which means that the release is informative about $g_d$. We interpret $g_d$ as a binary indicator bundling the prevailing monetary stance with the macro environment that supports it: in regime $H$, both the policy reaction to the state ($\theta_{x,H} > \theta_{x,L}$) and the typical level of the announcement ($\mu_H > \mu_L$) are higher than in regime $L$. The bundling captures the empirical regularity that aggressive policy stances coincide with elevated readings on the underlying macro indicator: a high-inflation regime is one in which CPI prints typically run above target *and* the Federal Reserve responds more forcefully to inflation deviations. The two channels of regime influence are precisely what makes $a_d$ diagnostic about $g_d$ in the first place; if $\mu_H = \mu_L$, the announcement carries no information about the policy slope.

Finally, a public macroeconomic announcement $a_d$ is released on day $d$, and $J$ private signals of the release are collected on day $d-1$ and aggregated into a consensus forecast.

**State process.** The macroeconomic fundamental follows a stationary AR(1) with release-specific long-run mean $\bar{x}^k$:

$$x_d = (1-\rho)\bar{x}^k + \rho x_{d-1} + \sigma_\varepsilon \varepsilon_d, \quad |\rho| < 1.$$

Here $x_d$ is the macro indicator in level form, and $\bar{x}^k$ is its unconditional mean. For the procyclical releases we study (nonfarm payrolls, CPI inflation, GDP, retail sales, and durable goods orders), $\bar{x}^k > 0$ in our sample, so $E[x_d] = \bar{x}^k > 0$ and the filtered state $x_{d|m}$ inherits this positive unconditional mean. It follows that the conditional mean of the cumulative discounted future state, $\mu_{X,h} \equiv E_d[X_h]$, also has positive unconditional mean for procyclical releases: along the slope-learning channel of (25), the average contribution is proportional to $\mathcal{B}_h \bar{x}^k > 0$. Initial claims, the lone countercyclical release, enters with reversed sign in the empirical specification, following the standard countercyclical-surprise convention; its slope-learning channel carries the opposite sign. This distinction matters in Section 5.6, where the sign of the slope-learning channel tracks the sign of $x_{d|m}$.

**Policy regime.** The short rate on day $d$ depends on the lagged short rate and the current state, with a regime-dependent sensitivity:

$$r_d = \phi r_{d-1} + \theta_{x,g_d}\, x_d + \eta_d, \quad \eta_d \sim N(0, \sigma_\eta^2), \tag{4}$$

where $\theta_{x,g_d} \in \{\theta_{x,H}, \theta_{x,L}\}$ with $\theta_{x,H} > \theta_{x,L}$ and

$$\Delta\theta_x \equiv \theta_{x,H} - \theta_{x,L} > 0.$$

Agents hold a prior $p_{d-1} = P(g_d = H \mid \mathcal{F}_{d-1})$ over the regime. Slope uncertainty (the variance of the policy slope given $\mathcal{F}_{d-1}$) is

$$SU_{d-1} \equiv \mathrm{Var}(\theta_{x,g_d} \mid \mathcal{F}_{d-1}) = p_{d-1}(1-p_{d-1})(\Delta\theta_x)^2,$$

which follows from the fact that $\theta_{x,g_d} = \theta_{x,L} + I_H \Delta\theta_x$ with $I_H \sim \text{Bernoulli}(p_{d-1})$.

**Announcement.** The public macroeconomic announcement depends on the latent state and the policy regime, with the regime shifting its conditional mean:

$$a_d = x_d + \mu_{g_d} + u_d, \quad u_d \sim N(0, \sigma_u^2), \tag{5}$$

with $\mu_H - \mu_L \equiv \Delta\mu \geq 0$. Without loss of generality, we normalize $\mu_H = \Delta\mu/2$ and $\mu_L = -\Delta\mu/2$. Two properties follow. First, the announcement carries information about the state $x_d$ through the $x_d$-term, independently of the regime. Second, because $\mu_{g_d}$ shifts the mean of $a_d$, the announcement also carries information about the regime: high prints are more likely under $H$ than under $L$. When $\Delta\mu = 0$, the release is purely state-informative and there is no slope learning; when $\Delta\mu > 0$, a single release both updates beliefs about $x_d$ (state learning) and about $g_d$ (slope learning). The two channels operate simultaneously, and their relative strength is governed by $\Delta\mu/\sigma_u^2$.

Equivalently, the subjective predictive distribution of the announcement after observing the consensus can be written as a two-component Gaussian mixture with weights $p_{d-1}$ and $1 - p_{d-1}$, a representation we exploit in Section 5.5.

**Consensus forecast.** On day $d-1$, $J$ forecasters submit private signals that are averaged into a public consensus forecast $m_{d-1}$. The cross-sectional variance of those signals is observed disagreement $\mathcal{D}_{d-1}$. Details are developed in Section 5.2.

**Timeline.** The day $d-1$ information set $\mathcal{F}_{d-1}$ contains the consensus forecast, forecasts disagreement and all prior public information; the day $d$ information set $\mathcal{F}_d$ adds the announcement. Agents update beliefs about $x_d$ twice (once after the consensus, once after the release) and about $g_d$ once (after the release).

In summary, two sources of noise affect learning but operate through distinct channels. The noise $u_d$ makes the announcement itself a noisy signal of the true state $x_d$. The private-signal noise, on the other hand, makes the consensus forecast $m_{d-1}$ a noisy pre-announcement signal of $x_d$, and it is this noise that drives observed disagreement $\mathcal{D}_{d-1}$. By contrast, short-rate uncertainty (the conditional variance of future short rates) depends on slope uncertainty (and hence on the prior $p_{d-1}$ over the regime), as well as on uncertainty about the future state of the economy and future shocks; see Section 5.4.

### 5.2 Day $d-1$: Consensus, Disagreement, and Filtering

Agents enter day $d-1$ with a common Gaussian prior on $x_d$: mean $x_{d|d-1}$ and variance $P_{d|d-1}$. During the day, $J$ forecasters each submit a private signal $z_{i,d-1} = x_d + c_{M_{i,d-1}} + \varepsilon_{i,d-1}$, where $c_{M_{i,d-1}}$ is a model-specific bias and $\varepsilon_{i,d-1} \sim N(0, \sigma^2_{\varepsilon,d-1})$ is idiosyncratic noise. The public consensus forecast is the average, $m_{d-1} = J^{-1}\sum_i z_{i,d-1}$, and *observed disagreement* $\mathcal{D}_{d-1}$ is the cross-sectional variance of the individual forecasts.

For the filtering problem, what matters is not how forecasters differ from each other (which is $\mathcal{D}_{d-1}$) but how much the consensus deviates from the truth (which is $\tilde{\mathcal{D}}_{d-1} \equiv \mathrm{Var}(m_{d-1} - x_d \mid \mathcal{F}_{d-1})$). Two forces separate these objects. First, averaging across $J$ iid noise draws shrinks the within-model component of consensus-error variance at rate $1/J$. Second, between-model heterogeneity is *correlated* across forecasters sharing a model, so its contribution to the consensus error does not shrink at rate $1/J$. We parameterize the share of observed disagreement attributable to between-model heterogeneity by a constant $\lambda \in [0,1]$ (treated as constant for tractability) and assume that the between-model contribution to the consensus-error variance is proportional to the between-model component, with scalar $\omega > 0$. Together these yield

$$\tilde{\mathcal{D}}_{d-1} = \omega\lambda\,\mathcal{D}_{d-1} + \frac{(1-\lambda)}{J}\mathcal{D}_{d-1}. \tag{6}$$

The full derivation of (6) is in Appendix A.1. The key takeaway is that $\partial\tilde{\mathcal{D}}_{d-1}/\partial\mathcal{D}_{d-1} > 0$: higher observed disagreement implies a noisier consensus as a signal of the fundamental.

Given $\tilde{\mathcal{D}}_{d-1}$, the standard Kalman update for a Gaussian signal gives the posterior for $x_d$ after seeing the consensus:

$$x_{d|m} = x_{d|d-1} + K_{m,d-1}(m_{d-1} - x_{d|d-1}), \qquad K_{m,d-1} = \frac{P_{d|d-1}}{P_{d|d-1} + \tilde{\mathcal{D}}_{d-1}}, \tag{7}$$

with posterior variance $P_{d|m} = (1 - K_{m,d-1})P_{d|d-1}$. A noisier consensus (larger $\tilde{\mathcal{D}}_{d-1}$) lowers the Kalman gain, so agents lean more on the prior and less on $m_{d-1}$; equivalently, a noisier consensus leaves more residual state uncertainty for the day-$d$ release to resolve.

### 5.3 Day $d$: The Announcement and Two Notions of Surprise

On the event day $d$, agents observe the announcement $a_d = x_d + \mu_{g_d} + u_d$ from (5). The econometrician and the agent face two distinct measures of surprise.

The observed (or measured) surprise is $s_d = a_d - m_{d-1}$, the familiar event study object. The

structural surprise is $\hat{s}_d = a_d - x_{d|m}$, the component of the release that is orthogonal to agents' information immediately before the release. These differ because the consensus is itself a noisy signal of $x_d$: the gap $m_{d-1} - x_{d|m}$ represents priors "catching up" with the consensus and is embedded in $s_d$ but not $\hat{s}_d$. Working through the algebra (Appendix A.2) delivers the useful identity

$$\hat{s}_d = s_d + (1 - K_{m,d-1})(m_{d-1} - x_{d|d-1}). \tag{8}$$

The wedge between the two surprises is proportional to the informational content of the consensus relative to the prior, scaled by $1 - K_{m,d-1}$. When the consensus is very informative ($K_{m,d-1} \approx 1$) the two surprises coincide; when the consensus is uninformative ($K_{m,d-1} \approx 0$), $s_d$ and $\hat{s}_d$ can differ substantially. Importantly, $\hat{s}_d$ is a martingale-difference sequence: $E[\hat{s}_d \mid \mathcal{F}_{d-1}] = 0$.

After observing the release, agents perform two parallel updates. The state update is a standard Kalman step:

$$x_{d|d} = x_{d|m} + K_{y,d}\hat{s}_d, \quad K_{y,d} = \frac{P_{d|m}}{P_{d|m} + \sigma_u^2}. \tag{9}$$

The regime update is a Bayesian revision of $p_{d-1}$ in light of the release, described in Section 5.5. The Kalman gain $K_{y,d}$ uses the *regime-conditional* residual variance: given $g_d$, the announcement noise has variance $\sigma_u^2$. The unconditional residual variance is larger, $P_{d|m} + \sigma_u^2 + p_{d-1}(1 - p_{d-1})(\Delta\mu)^2$, with the additional regime-mean uncertainty absorbed into the separate Bayesian regime update of Section 5.5. Equivalently, (9) together with the regime update is the two-step linearization, around $\hat{s}_d = 0$, of the exact Gaussian-mixture posterior on $(x_d, g_d)$ given $a_d$. The joint posterior is identified — there is no observational equivalence between "high state" and "high regime," since the joint likelihood pins down both — and the gap between sequential and joint updates is $O(\hat{s}_d^2)$, small for typical surprise magnitudes (Appendix A.4).

### 5.4 Short Rate Uncertainty

The short-rate uncertainty $SRU_{d-1,h} \equiv \mathrm{Var}(r_{d+h} \mid \mathcal{F}_{d-1})$ is a composite object: it aggregates uncertainty about the future policy slope, the future state, and future shocks. Making this decomposition explicit is useful because it is slope uncertainty (not total $SRU$) that drives the slope-learning channel in the yield response below.

Iterating the policy rule (4) forward and invoking an anticipated utility assumption (agents treat the currently perceived policy sensitivity as applying at all future horizons, $\theta_{x,g_{d+k}} \approx \theta_{x,g_d}$ for

$k \geq 0$), the short-rate uncertainty decomposes as

$$SRU_{d-1,h} = \underbrace{\sigma^2_{\theta,d-1}(\sigma^2_{X,h} + \mu^2_{X,h})}_{\text{slope} \times \text{state}} + \underbrace{(\bar{\theta}^{d-1}_x)^2 \, \sigma^2_{X,h}}_{\text{state uncertainty}} + \underbrace{\sum_{j=0}^{h} \phi^{2(h-j)} \sigma^2_\eta}_{\text{shock uncertainty}}, \tag{10}$$

where $\mu_{X,h}$ and $\sigma^2_{X,h}$ are the conditional mean and variance of the cumulative discounted future state, $X_h \equiv \sum_{j=0}^{h} \phi^{h-j} x_{d+j}$, and where $\bar{\theta}^{d-1}_x$ and $\sigma^2_{\theta,d-1}$ are the mean and variance of the regime-dependent slope $\theta_{x,g_d}$ given $\mathcal{F}_{d-1}$. The derivation, including the product-of-random-variables variance formula, is collected in Appendix A.3.

Two features of (10) matter for what follows. First, the slope-uncertainty term $\sigma^2_{\theta,d-1}$ equals $SU_{d-1} = p_{d-1}(1 - p_{d-1})(\Delta\theta_x)^2$: it scales with the gap between the regimes and peaks when the prior is balanced ($p_{d-1} = 1/2$). Second, $SRU_{d-1,h}$ conflates slope uncertainty with state and shock uncertainty, so it is not identical to $SU_{d-1}$; the intercept and loading in the reduced-form regressions of Section 5.8 are affected accordingly.

### 5.5 Release Informativeness and Posterior Beliefs

The DGP (5) implies a Gaussian mixture predictive distribution for $a_d$, with regime-conditional means $x_{d|m} \pm \Delta\mu/2$ and common variance $\sigma^2_a \equiv P_{d|m} + \sigma^2_u$. Applying Bayes' rule to this two-Gaussian mixture and taking logs, the posterior regime log-odds are linear in the structural surprise (see Appendix A.4 for the full derivation):

$$\log \frac{p_d}{1 - p_d} = \log \frac{p_{d-1}}{1 - p_{d-1}} + \kappa \, \hat{s}_d, \qquad \kappa \equiv \frac{\Delta\mu}{\sigma^2_a}. \tag{11}$$

The slope $\kappa$ is the *diagnostic content* of the release. It rises with $\Delta\mu$ (a bigger mean shift between regimes means the release is a sharper test of which regime prevails) and falls with $\sigma^2_a$ (a noisier predictive distribution makes the release less decisive). The log-odds representation is natural: each release adds a constant multiple of $\hat{s}_d$ to the current regime log-odds, exactly as in a sequential Bayesian classification problem.

A first-order Taylor expansion of (11) around $\hat{s}_d = 0$ gives the useful approximation

$$\frac{\partial p_d}{\partial a_d} \approx p_{d-1}(1 - p_{d-1}) \, \kappa. \tag{12}$$

The marginal revision in the regime probability scales with three factors: prior regime uncertainty (largest at $p_{d-1} = 1/2$), the mean shift $\Delta\mu$, and the inverse predictive variance $1/\sigma^2_a$. The

approximation is accurate when $p_{d-1}$ is near $1/2$ and $\hat{s}_d$ is small; the detailed bound is in Appendix A.4.

**Expected reduction in slope uncertainty.** Applying the law of total variance to $\theta_{x,g_d}$ (Appendix A.4) yields

$$E[SU_d \mid \mathcal{F}_{d-1}] = SU_{d-1} - (\Delta\theta_x)^2 \operatorname{Var}(p_d \mid \mathcal{F}_{d-1}) \leq SU_{d-1}. \tag{13}$$

The release always weakly reduces slope uncertainty on average, and the reduction is larger when the prior is balanced and the release is diagnostic. When $\Delta\mu = 0$, the release carries no regime information ($\operatorname{Var}(p_d \mid \mathcal{F}_{d-1}) = 0$) and slope uncertainty is unchanged. Importantly, higher forecast disagreement raises $P_{d|m}$ and therefore $\sigma_a^2$, shrinking $\kappa$ and limiting slope learning – a connection we exploit when analyzing the disagreement effect below.

Higher consensus noise raises $P_{d|m}$ and hence $\sigma_a^2$, shrinking $\Delta\mu/\sigma_a^2$ and limiting learning about the regime. Higher forecast disagreement therefore dampens the reduction in short-rate uncertainty on release days, a testable prediction of the model.

### 5.6 Response of Yields to Announcements

Under risk-neutral pricing, the change in the $h$-period futures rate around the announcement equals the revision in the expected short rate, $\Delta E_d[r_{d+h}]$. Gürkaynak, Kısacıkoğlu, and Wright (2020) document that the bulk of the Treasury-yield response to macro news surprises is concentrated in the expectations component, with the term premium component accounting for a small share, and Hördahl, Remolona, and Valente (2020) reach the same conclusion in a complementary affine term structure decomposition: yield reactions to macro news are primarily driven by revisions in short rate expectations, with risk premium adjustments contributing a smaller and partially offsetting effect. The model accordingly isolates this dominant expectations channel and treats the term-premium component as second-order at the 20-minute event-window frequency. This revision is nonlinear in $\hat{s}_d$ because the structural surprise simultaneously revises beliefs about the state $x_d$ (via a Kalman update) and about the regime $g_d$ (via the logistic Bayes rule in (11)). Linearizing the revision around $\hat{s}_d = 0$ (see Appendix A.5) delivers the central yield-response coefficient of the paper:

$$\beta(\hat{s}_d) \equiv \frac{\partial E_d[r_{d+h}]}{\partial \hat{s}_d} = \underbrace{G_h(\phi,\rho)\,\bar{\theta}_x^{d-1}\,K_{y,d}}_{\text{state-learning channel}} + \underbrace{\frac{SU_{d-1}}{\Delta\theta_x}\,\frac{\Delta\mu}{\sigma_a^2}\,\mu_{X,h}}_{\text{slope-learning channel}}, \tag{14}$$

where $G_h(\phi, \rho) \equiv \sum_{j=0}^{h} \phi^{h-j}\rho^j$ is the discounted AR(1) state loading and $K_{y,d} = P_{d|m}/(P_{d|m} + \sigma_u^2)$ is the announcement Kalman gain.

Equation (14) delivers the model's two core predictions. The first prediction is based on the state learning channel. The first term scales with the announcement Kalman gain $K_{y,d}$. When the pre-release prior about $x$ is diffuse ($P_{d|m}$ large), the announcement carries more information about the state and moves expected future short rates more strongly. This is the standard learning mechanism: diffuse priors yield large updates. The second prediction is based on the effects of the slope learning channel.The second term scales with slope uncertainty $SU_{d-1}$ times diagnostic content $\Delta\mu/\sigma_a^2$ times the pre-release expected state path $\mu_{X,h}$. The logic is multiplicative: slope uncertainty sets how much the perceived policy sensitivity $\bar{\theta}_x$ can move; diagnostic content sets how sharply a given surprise updates the regime probability; and $\mu_{X,h}$ scales the consequences, because a revision in $\bar{\theta}_x$ moves expected future short rates by $\Delta\bar{\theta}_x \cdot \mu_{X,h}$. The channel reinforces state-learning when the state is expected above steady state ($\mu_{X,h} > 0$) and partially offsets it when the state is expected below. The slope learning channel is the mechanism through which higher short-rate uncertainty amplifies yield responses: $SU_{d-1}$ is the specific component of $SRU_{d-1,h}$ that enters $\beta(\hat{s}_d)$. Section 5.8 makes this mapping explicit.

### 5.7 From Structural to Measured Surprise: Attenuation

Equation (14) gives the yield response to the *structural* surprise $\hat{s}_d$, but empirical event studies regress yield changes on the *measured* surprise $s_d = a_d - m_{d-1}$. Because $\Delta E_d[r_{d+h}]$ is a linear function of $\hat{s}_d$, the observed event-study coefficient factors as

$$\beta(s_d) = \beta(\hat{s}_d) \cdot \mathcal{A}_d, \qquad \mathcal{A}_d \equiv \frac{\text{cov}(s_d, \hat{s}_d)}{\text{var}(s_d)}. \tag{15}$$

The factor $\mathcal{A}_d$ captures the classical measurement error attenuation: $s_d$ is a noisy proxy for $\hat{s}_d$ because the consensus noise $\xi_{d-1} \equiv m_{d-1} - x_d$ enters $s_d$ one-for-one but has already been partially absorbed into $x_{d|m}$, so only the residual portion $K_{m,d-1}\xi_{d-1}$ survives in $\hat{s}_d$.

A direct covariance calculation (Appendix A.6) yields the closed-form

$$\mathcal{A}_d = \frac{\sigma_u^2 + K_{m,d-1}\tilde{\mathcal{D}}_{d-1}}{\sigma_u^2 + \tilde{\mathcal{D}}_{d-1}} \in [0, 1]. \tag{16}$$

When the consensus is perfectly informative ($K_{m,d-1} = 1$ or $\tilde{\mathcal{D}}_{d-1} = 0$), $\mathcal{A}_d = 1$ and observed and structural surprises coincide. When the consensus is uninformative, $\mathcal{A}_d$ collapses toward

$\sigma_u^2/(\sigma_u^2 + \tilde{\mathcal{D}}_{d-1})$, and the observed coefficient is heavily shrunk toward zero.

### 5.8 Analytical Results

We now combine the structural surprise coefficient $\beta(\hat{s}_d)$ in (14) and the attenuation factor $\mathcal{A}_d$ in (16) to characterize how the observed coefficient $\beta(s_d) = \mathcal{A}_d\,\beta(\hat{s}_d)$ responds to the two empirical regressors of interest: short-rate uncertainty $SRU_{d-1,h}$ and observed disagreement $\mathcal{D}_{d-1}$. By construction, disagreement does not affect slope uncertainty (and vice versa), so the marginal effects are conceptually distinct.

**Short rate uncertainty effect.** Because (10) bundles slope uncertainty with state and shock uncertainty, we rewrite $\beta(\hat{s}_d)$ as a direct function of $SRU_{d-1,h}$ by solving (10) for $\sigma^2_{\theta,d-1}$ and substituting into (14) (Appendix A.7):

$$\beta_h(\hat{s}_d) = C_{d,h}(\tilde{\mathcal{D}}_{d-1}) + \Lambda_{d,h}\,SRU_{d-1,h}, \tag{17}$$

where

$$\Lambda_{d,h} \equiv \frac{\Delta\mu}{\sigma_a^2}\,\frac{\mu_{X,h}}{\Delta\theta_x(\sigma^2_{X,h} + \mu^2_{X,h})}, \tag{18}$$

and the intercept $C_{d,h}(\tilde{\mathcal{D}}_{d-1})$ collects the state learning and shock variance terms. Multiplying through by $\mathcal{A}_d$ yields the observed coefficient:

$$\beta_h(s_d) = \mathcal{A}_d(\tilde{\mathcal{D}}_{d-1})\left[C_{d,h}(\tilde{\mathcal{D}}_{d-1}) + \Lambda_{d,h}\,SRU_{d-1,h}\right]. \tag{19}$$

The loading $\Lambda_{d,h}$ is the model's prediction for the reduced form slope on $SRU$ in the event study regression. It is positive when $\mu_{X,h} > 0$ and rises with diagnostic content $\Delta\mu/\sigma_a^2$. Intuitively, a given increase in $SRU_{d-1,h}$ produces a larger yield response exactly when the release is informative about the regime and the pre-release state is expected away from steady state.

**Disagreement effect.** Differentiating (19) with respect to $\mathcal{D}_{d-1}$, holding $SRU_{d-1,h}$ fixed, and applying the chain rule, the sign of the disagreement effect is determined by the balance of two opposing forces (Appendix A.7). The attenuation channel, given by $\mathcal{A}'_d(\tilde{\mathcal{D}}_{d-1}) < 0$, implies that a more dispersed consensus makes $s_d$ a noisier proxy for $\hat{s}_d$, mechanically shrinking $\beta(s_d)$ toward zero. On the other hand the structural amplification channel implies that a more dispersed consensus raises the residual state uncertainty $P_{d|m}$, which raises the announcement Kalman gain $K_{y,d}$ and

amplifies the structural response. Because these two channels pull in opposite directions, the overall disagreement effect is indeterminate without further restrictions. The next subsection provides a closed-form characterization that pins down exactly when each channel dominates.

### 5.9 Closed-Form Characterization of the Disagreement Effect

The sufficient conditions derived above involve several derivative terms that are difficult to sign in general. We now provide a closed-form characterization that pins down the exact threshold at which the disagreement effect changes sign.

**Proposition 1** *The product of the attenuation factor and the announcement Kalman gain admits the closed form:*

$$\mathcal{A}_d \cdot K_{y,d} = \frac{P_{d|d-1}\,\tilde{\mathcal{D}}_{d-1}}{(\sigma_u^2 + \tilde{\mathcal{D}}_{d-1})(P_{d|d-1} + \tilde{\mathcal{D}}_{d-1})} \tag{20}$$

*This product is hump-shaped in $\tilde{\mathcal{D}}_{d-1}$, with a unique interior maximum at*

$$\tilde{\mathcal{D}}^* = \sigma_u \sqrt{P_{d|d-1}} \tag{21}$$

*In particular,*

$$\frac{\partial(\mathcal{A}_d \cdot K_{y,d})}{\partial \tilde{\mathcal{D}}_{d-1}} \gtrless 0 \iff \tilde{\mathcal{D}}_{d-1} \lessgtr \tilde{\mathcal{D}}^*$$

See Appendix A.8.

The result sharply characterizes the disagreement effect. Abstracting from slope learning ($\mu_{X,h} = 0$ or $\Delta\mu = 0$), the observed surprise coefficient reduces to $\beta_h(s_d) = \mathcal{A}_d \cdot G_h(\phi, \rho) \cdot \bar{\theta}_x^{d-1} \cdot K_{y,d}$. Since $G_h(\phi, \rho)$ and $\bar{\theta}_x^{d-1}$ do not depend on $\tilde{\mathcal{D}}_{d-1}$, the sign of $\partial\beta_h(s_d)/\partial\mathcal{D}_{d-1}$ is pinned down entirely by the sign of $\partial(\mathcal{A}_d \cdot K_{y,d})/\partial\tilde{\mathcal{D}}_{d-1}$, which flips at the threshold $\tilde{\mathcal{D}}^* = \sigma_u\sqrt{P_{d|d-1}}$.

The threshold $\tilde{\mathcal{D}}^*$ separates two regimes for the effect of disagreement on the yield response to announcements. When the consensus error variance is small relative to the threshold ($\tilde{\mathcal{D}}_{d-1} < \tilde{\mathcal{D}}^*$), an *information effect* operates. Higher disagreement primarily increases residual uncertainty about the state $x_d$ after observing the consensus, which raises the informativeness of the subsequent announcement and increases $K_{y,d}$. The increase in the structural surprise coefficient $\beta_h(\hat{s}_d)$ dominates the decline in the attenuation factor $\mathcal{A}_d$, so the observed-surprise coefficient $\beta_h(s_d)$ rises with disagreement.

When the consensus error variance is large ($\tilde{\mathcal{D}}_{d-1} > \tilde{\mathcal{D}}^*$), an *attenuation effect* takes over. The Kalman gain $K_{y,d}$ is already close to its upper bound $P_{d|d-1}/(P_{d|d-1} + \sigma_u^2)$ and responds only weakly

to further increases in $\tilde{\mathcal{D}}_{d-1}$. Meanwhile, the attenuation factor $\mathcal{A}_d$ continues to decline because the measured surprise $s_d = u_d - \xi_{d-1}$ becomes an increasingly noisy proxy for the structural surprise $\hat{s}_d$. Attenuation dominates, and $\beta_h(s_d)$ falls with disagreement.

The threshold $\tilde{\mathcal{D}}^* = \sigma_u \sqrt{P_{d|d-1}}$ is the geometric mean of announcement noise variance and state prediction variance. The two effects balance when the consensus error variance equates the product of the two other sources of uncertainty in the system.

The empirical finding that higher disagreement lowers the yield response requires $\tilde{\mathcal{D}}_{d-1} > \sigma_u \sqrt{P_{d|d-1}}$ for the typical observation. This imposes a joint restriction: either announcement noise $\sigma_u^2$ must be small relative to $\tilde{\mathcal{D}}_{d-1}$, or $P_{d|d-1}$ must be small enough that the information channel is already saturated. For macroeconomic data releases, where announcements are typically precise relative to forecast dispersion, the attenuation regime is the empirically relevant one.

### 5.10 Time-Varying Signal Precision and the CPI/NFP Distinction

The baseline framework treats the signal-precision parameters $(\Delta\mu, \sigma_u^2)$ as time-invariant within a release. The empirical results in Section 4 show that $\hat{\beta}^k_{5,n}$, the SRU interaction coefficient, moved in opposite directions for CPI and NFP across the pre-2020 and post-COVID subsamples: positive and significant for CPI post-COVID (after being indistinguishable from zero pre-2020), and shrinking by roughly half toward insignificance for NFP. The baseline model with constant parameters cannot generate this pattern. We extend it to allow release-specific, time-varying signal precision $(\Delta\mu_t^k, \sigma_{u,t}^{2,k})$ for each release $k$ at date $t$, and write $\sigma_{a,t}^{2,k} \equiv P_{d|m} + \sigma_{u,t}^{2,k}$ for the corresponding predictive variance.

Equation (18) delivers the comparative statics directly. Decomposing the loading on $SRU$,

$$\Lambda^k_{d,h} = \underbrace{\frac{\Delta\mu_t^k}{\sigma_{a,t}^{2,k}}}_{\text{diagnostic content}} \cdot \underbrace{\frac{\mu_{X,h}}{\Delta\theta_x(\sigma^2_{X,h} + \mu^2_{X,h})}}_{\text{state-path geometry}}, \tag{22}$$

the first factor captures release- and date-specific diagnosticity, while the second is common across releases and depends only on the state dynamics. With $\mu_{X,h} > 0$ in our sample (Section 5.1),

$$\frac{\partial \Lambda^k_{d,h}}{\partial \Delta\mu_t^k} > 0, \qquad \frac{\partial \Lambda^k_{d,h}}{\partial \sigma_{u,t}^{2,k}} < 0.$$

The post-2021 inflation surge widened the regime-conditional separation in CPI announcements. With inflation persistently five to seven percentage points above target, the realized distance between

the high policy response regime (in which inflation is elevated and the Federal Reserve responds aggressively) and the low-policy-response regime (in which inflation is anchored and policy is accommodative) became larger than it had been since the early 1980s. In the model this is captured as an increase in $\Delta\mu_t^{\text{cpi}}$: the gap $\mu_H - \mu_L$ in the conditional mean of CPI announcements widened, so each CPI print became a sharper signal of which regime obtains. The diagnostic-content factor in (22) rises, lifting $\Lambda_{d,h}^{\text{cpi}}$ and predicting the positive and significant CPI $\times$ SRU interaction documented in Table 2 Panel C and the structural-break test in Table 3 Panel A.

Two precision channels move in the opposite direction for payrolls. First, $\sigma_{u,t}^{2,\text{nfp}}$ rose mechanically: the response rate of the BLS Current Employment Statistics survey fell from roughly 60% pre-pandemic to under 45% afterward (Leduc, Oliveira, and Paulson (2025)), and the August 2024 preliminary annual benchmark revision reduced the reported level of nonfarm payrolls by approximately 818,000 jobs for the twelve months ending March 2024, the largest such downward revision since 2009. Second, $\Delta\mu_t^{\text{nfp}}$ declined as CPI displaced NFP as the marginal signal about the rate path. Both forces shrink the diagnostic content of NFP releases and thus $\Lambda_{d,h}^{\text{nfp}}$, predicting the attenuation of the NFP $\times$ SRU interaction observed in Table 2 Panel C and confirmed by the negative shift coefficient in Table 3 Panel B.

The same precision shifts also enter the attenuation factor $\mathcal{A}_d$ in (16), since $\sigma_{u,t}^{2,k}$ appears directly in the numerator and denominator. A higher $\sigma_{u,t}^{2,\text{nfp}}$ raises $\sigma_{a,t}^{2,\text{nfp}}$ and dampens the disagreement-driven attenuation channel as well. The model therefore predicts that the NFP $\times$ disagreement coefficient should collapse alongside NFP $\times$ SRU — consistent with the roughly fifty-fold drop in NFP $\times$ disagreement documented in Table 2 Panel B. The same precision shifts therefore explain the joint behavior of both interaction terms within a single mechanism, without requiring separate explanations for SRU and disagreement.

# 6 Calibration and Simulation

To gauge the quantitative implications of the model, we simulate announcement histories from the data generating process, and compare the model-implied yield response coefficients to event study regressions estimated on the simulated data.

## 6.1 From Futures to Yields

The analytical results above are stated in terms of the futures rate at horizon $h$, $E_d[r_{d+h}]$. In practice, the objects of interest are zero-coupon bond yields, which under risk-neutral pricing equal the

average of expected future short rates:

$$y_d^{(h)} = \frac{1}{h} \sum_{\tau=1}^{h} E_d[r_{d+\tau}]$$

The change in the $h$-maturity yield around the announcement is therefore:

$$\Delta y_d^{(h)} = \frac{1}{h} \sum_{\tau=1}^{h} \Delta E_d[r_{d+\tau}] \tag{23}$$

For each horizon $\tau$, the futures rate loading on the state is $G_\tau(\phi, \rho) = \sum_{j=0}^{\tau} \phi^{\tau-j} \rho^j$. The corresponding yield loading is the average across horizons (see Section B for details):

$$\mathcal{B}_h(\phi, \rho) = \frac{1}{h} \sum_{\tau=1}^{h} G_\tau(\phi, \rho) \tag{24}$$

When $|\phi| < 1$ and $|\rho| < 1$, the futures loading $G_h$ converges to zero as $h \to \infty$, so futures rate responses vanish at long horizons. The yield loading $\mathcal{B}_h$, by contrast, averages over all horizons from 1 to $h$, including the short ones where $G_\tau$ is large, and therefore remains economically meaningful even at 10-year maturities.

The yield-response coefficient to the structural surprise then takes the same form as before, with $G_h$ replaced by $\mathcal{B}_h$:

$$\beta_h^{\text{yield}}(\hat{s}_d) = \underbrace{\mathcal{B}_h(\phi, \rho)\, \bar{\theta}_x^{d-1}\, K_{y,d}}_{\text{State learning}} + \underbrace{\Delta\theta_x \frac{\partial p_d}{\partial \hat{s}_d}\, \mu_{X,h}^{\text{yield}}}_{\text{Slope learning}} \tag{25}$$

where $\mu_{X,h}^{\text{yield}} = \mathcal{B}_h \cdot x_{d|m}$. The observed-surprise coefficient is $\beta_h^{\text{yield}}(s_d) = \mathcal{A}_d \cdot \beta_h^{\text{yield}}(\hat{s}_d)$, with the attenuation factor $\mathcal{A}_d$ unchanged.

### 6.2 Calibration

Table 4 reports the parameter values. The calibration is chosen to illustrate the model's qualitative properties rather than to match specific data moments.

The state process is highly persistent ($\rho = 0.995$), generating substantial variation in the pre-announcement conditional mean $x_{d|m}$. The regime separation $\Delta\theta_x = \theta_{x,H} - \theta_{x,L} = 1.0$ is large enough to produce meaningful slope uncertainty, and $\Delta\mu = 2.0$ implies that releases are informative about the regime, enabling slope learning.

The key calibration choice is $\sigma_u = 0.10$, which is small relative to the consensus error variance

$\tilde{\mathcal{D}}_{d-1}$. This places the model in the attenuation-dominated regime of Proposition 1: since $\tilde{\mathcal{D}}_{d-1} > \sigma_u \sqrt{P_{d|d-1}} = \tilde{\mathcal{D}}^*$ for the typical observation, higher disagreement lowers the observed surprise coefficient, consistent with the empirical evidence. A larger $\sigma_u$ (e.g., $\sigma_u = 0.50$) would push $\tilde{\mathcal{D}}^*$ above typical disagreement levels, producing the counterfactual prediction that disagreement raises yield responses.

Yield maturities are 2, 5, and 10 years (504, 1260, and 2520 business days). As discussed in Section 6.1, we use the yield loading $\mathcal{B}_h$ rather than the futures loading $G_h$, which ensures meaningful responses at long maturities.

### 6.3 Simulation Results

We draw 5000 announcement days from the data-generating process, run the two-stage Kalman filter and the Bayesian regime learning recursion to construct agents' real time beliefs, and compute the analytical yield response coefficients $\beta_h^{\text{yield}}(\hat{s}_d)$ and $\beta_h^{\text{yield}}(s_d)$ for each day and maturity alongside the simulated yield changes $\Delta y_d^{(h)}$. Results are reported in Figures 7–10.

**Short rate uncertainty and yield responses.** Recall that the model predicts $\beta_h(\hat{s}_d) = C_{d,h} + \Lambda_{d,h} \cdot SRU_{d-1,h}$, where the intercept and slope vary across observations through the prior $p_{d-1}$, the consensus error variance $\tilde{\mathcal{D}}_{d-1}$, the Kalman gain $K_{y,d}$, and the pre-announcement conditional mean $x_{d|m}$. Figure 7 plots the observation-level pairs $(SRU_{d-1,h},\ \beta_h^{\text{yield}})$ for each maturity, overlaid with OLS fit lines and binned event-study estimates from the simulated yield data.

The OLS slope is positive at all three maturities, confirming the model's central prediction that days with higher short-rate uncertainty exhibit larger yield responses. The slope for the structural surprise beta increases from 2.10 at 2 years to 4.82 at 5 years and 9.63 at 10 years; the corresponding observed surprise slopes are 1.28, 2.94, and 5.87, reflecting the attenuation wedge. That $\Lambda$ increases with maturity is intuitive: the slope-learning channel operates through revisions to the expected policy regime, whose cumulative impact on the rate path grows with the horizon. The binned event study estimates track the OLS lines closely, validating the first-order approximation underlying the analytical $\beta$ expressions.

**Disagreement and yield responses.** Figure 8 shows the comparative statics effect of disagreement on $\beta_h(s_d)$, evaluated at the median of all other state variables. Consistent with Proposition 1, the yield response coefficient declines with disagreement at all maturities. Moving from the 5th to the 95th percentile of observed disagreement, $\beta_h(s_d)$ falls by roughly 46%, while the attenuation

factor $\mathcal{A}_d$ drops by only 28%. The gap reflects a second channel: higher disagreement also raises the post-consensus variance $P_{d|m}$, which increases $\sigma_a^2$ and lowers the slope-learning term $(\Delta\mu/\sigma_a^2)$. Because the yield loading $\mathcal{B}_h$ enters as a common scale factor, the proportional decline is the same across maturities.

**Term structure and decomposition.** Figure 9 reports the average structural and observed surprise coefficients across maturities. Both decline along the term structure, reflecting the decay of $\mathcal{B}_h$: although the yield loading remains bounded away from zero (unlike $G_h$), it still falls because $\phi < 1$ implies that distant short rates are only weakly linked to current-period information. The ratio of the observed to the structural coefficient, the average attenuation factor, is roughly 0.60 and stable across maturities, since attenuation depends on the consensus error variance and announcement noise, neither of which varies with the horizon.

Figure 10 decomposes the average structural surprise coefficient into its two components from (25). Slope learning accounts for about 60% of the total at every maturity, with state learning contributing the remaining 40%. This split reflects the large regime separation ($\Delta\theta_x = 1.0$) and high diagnostic content ($\Delta\mu = 2.0$), which generate substantial belief revision about the policy regime on each announcement day. The state learning channel, while always active, is limited by the fact that $K_{y,d}$ is already close to its upper bound when $\sigma_u$ is small. Both components are proportional to $\mathcal{B}_h$, so the 60/40 decomposition is preserved along the term structure.

### 6.4 Structural Estimation: Time-Varying Signal Precision

We complement the calibration with a simulated method of moments (SMM) estimation that disciplines the key signal precision parameters using the empirical regression evidence directly. The estimation matches the main-surprise coefficient $\hat{\beta}_1$ and the surprise-by-SRU interaction coefficient $\hat{\beta}_5$ across four release-period blocks (NFP and CPI, pre-2020 and post-COVID) and three maturities (2-, 5-, and 10-year). We hold the announcement-noise standard deviations $\sigma_u^{\text{nfp}}$ and $\sigma_u^{\text{cpi}}$ at calibrated values and estimate six structural parameters: the period-specific policy reaction-function spreads $(\Delta\theta_x^{\text{pre}}, \Delta\theta_x^{\text{post}})$ and the four release-and-period-specific regime mean shifts $(\Delta\mu_{\text{pre}}^{\text{nfp}}, \Delta\mu_{\text{post}}^{\text{nfp}}, \Delta\mu_{\text{pre}}^{\text{cpi}}, \Delta\mu_{\text{post}}^{\text{cpi}})$. With twenty-four target moments and six free parameters, the system is over-identified by eighteen restrictions, providing strong cross-maturity discipline on the structural estimates. Standard errors are computed using the asymptotic SMM sandwich formula evaluated at the empirical regression-coefficient covariance. As is common in highly parameterized stylized macro models with many over-identifying restrictions, the overall SMM

$J$-statistic rejects the joint null of correct specification and optimal weighting; the economically informative diagnostics, on which we focus below, are the parameter-restriction Wald tests in Panel B of Table 5 and the targeted-versus-fitted moment comparisons in Panel C.

Table 5 reports the estimates. Three findings stand out. First, the structural parameters confirm the time-varying-precision mechanism of Section 5.10: the CPI regime-mean separation $\Delta\mu^{\text{cpi}}$ rises by more than two orders of magnitude across COVID (from 0.005 to 1.551), while the NFP regime-mean separation $\Delta\mu^{\text{nfp}}$ contracts by roughly thirty-five percent (from 0.886 to 0.574). Both shifts are highly significant by Wald tests based on asymptotic SMM standard errors. Second, the policy reaction-function spread is statistically indistinguishable across the two periods ($\Delta\theta_x^{\text{pre}} = 0.0196$ versus $\Delta\theta_x^{\text{post}} = 0.0200$, Wald $p = 0.53$). The post-COVID changes in yield-response patterns therefore operate entirely through release-specific signal precision rather than through changes in the latent monetary reaction function: the data are consistent with a stable policy slope spread combined with a dramatic reweighting of the diagnostic content of CPI relative to NFP. Third, the model captures the qualitative term-structure shape of the empirical surprise-by-SRU interaction $\hat{\beta}_5$ across all four blocks: the response declines with maturity in both data and model, consistent with the decay of the yield loading $\mathcal{B}_h$. The fit on the main-surprise coefficient $\hat{\beta}_1$ is closer at the 5- and 10-year maturities than at the 2-year maturity, where the empirical hump-shape is not generated by the single horizon factor $\mathcal{B}_h$ in the baseline model.[3] Formal moment-level tests reinforce this qualitative reading. For each of the twenty-four targeted moments we compute a two-sided $t$-statistic for the null that the model-implied moment equals its empirical counterpart, with standard error $\sigma_k\sqrt{1+1/\tau}$, where $\sigma_k$ is the empirical regression standard error and $\tau = N_{\text{sim}}/n_{\text{emp}}$ adjusts for simulation noise. Seventeen of the twenty-four moments are individually indistinguishable from their empirical targets after a family-wise five-percent Bonferroni correction across the twenty-four tests (critical value $|t| > 3.08$); the seven rejections are concentrated in $\hat{\beta}_1$—five rejections all reflecting the term-structure hump just discussed—and in the CPI $\times$ SRU interaction at the 5- and 10-year maturities post-COVID, where the model captures the sign and significance of the interaction but under-predicts its absolute magnitude. Ten of the twelve $\hat{\beta}_5$ moments—the economically central comparative-static targets for the time-varying-precision mechanism—are

[3] Reproducing the hump-shaped term structure of $\hat{\beta}_1$ would require an additional horizon-dependent channel beyond the yield loading $\mathcal{B}_h$. Three natural extensions could deliver this: a maturity-specific term premium that responds to announcements (consistent with the small but non-zero risk-premium component documented by Hördahl, Remolona, and Valente (2020)), maturity-specific market microstructure such as differential liquidity across the 2-, 5-, and 10-year futures contracts, or distinct horizon decay rates for the state-learning and slope-learning channels. We leave such extensions for future work; the qualitative direction of the structural shifts identified here—a stable policy reaction-function spread combined with a substantial reweighting of release-specific signal precision in favor of CPI—is preserved across the three maturities targeted by the estimation.

individually consistent with the model after Bonferroni correction, including all six NFP $\times$ SRU cells across both subsamples and all three pre-2020 CPI $\times$ SRU cells. The disagreement-interaction coefficient $\hat{\beta}_3$ is reported diagnostically only; the baseline framework abstracts from state-dependent variation in disagreement, leaving exact $\beta_3$ magnitudes for future extensions of the framework.

Taken together, the structural estimates point to a stable policy reaction-function spread across COVID, with the post-COVID changes in yield-response patterns operating entirely through changes in the diagnostic content of individual macro releases. This reading speaks to the recent literature on changes in market-perceived Federal Reserve reaction-function parameters around the inflation surge (Bauer, Pflueger, and Sunderam (2025), Xia and Zhu (2025)): the data are consistent with the view that what changed across COVID is the informational content of specific macroeconomic indicators rather than the underlying monetary reaction function itself.

## 7 Conclusion

This paper studies how two informational frictions, macroeconomic forecast disagreement and monetary policy uncertainty, shape the responsiveness of U.S. Treasury bond yields to macroeconomic data surprises. Using intraday data on Treasury futures around releases of CPI, nonfarm payrolls, initial claims, durable goods orders, retail sales, and GDP, we show that the yield curve's reaction to macro news varies systematically with the level of disagreement and policy uncertainty at the time of the announcement.

Greater forecast disagreement about a given release dampens the yield response, consistent with disagreement signaling lower informational content of that variable for future monetary policy. Higher short-rate uncertainty, by contrast, amplifies yield responses, consistent with macro surprises being more informative when policy expectations are diffuse. These patterns hold for most release types in the pre-2020 sample, with the notable exception that inflation surprises drew only weak responses even when short-rate uncertainty was high. The post-COVID period reveals two further departures from the pre-2020 pattern, in opposite directions: the CPI surprise response becomes positively conditional on short-rate uncertainty, while the nonfarm-payroll response loses its previously strong dependence on short-rate uncertainty.

We develop a Bayesian learning model to interpret these results. In the baseline framework, forecast disagreement reduces the signal-to-noise ratio of the public signal, attenuating yield responses. Short rate uncertainty magnifies the market response because announcement surprises carry more information about the trajectory of future interest rates when uncertainty about that

trajectory is high.

We extend the model to allow for time-varying precision of macroeconomic announcements, which lets a single mechanism rationalize both post-COVID departures. CPI precision rises post-COVID as the Fed's communicated emphasis on inflation makes CPI surprises more diagnostic about the rate path; the bond-market response to CPI is amplified by short-rate uncertainty for the first time in our sample. Payroll precision falls for several reasons: measurement noise (declining BLS Current Employment Statistics response rates and historically large annual benchmark revisions); structural dislocations in the labor market itself (pandemic exits, sectoral reallocation, and shifts in labor force participation); and CPI displacing payrolls as the marginal signal of policy direction. As a result, the bond-market response to NFP becomes effectively independent of short-rate uncertainty in the post-COVID period.

The bond market's sensitivity to macro announcements depends not only on the news itself but also on how informative that news is perceived to be. In US Treasury markets, accounting for disagreement and monetary policy uncertainty matters for interpreting yield responses to economic news.

# Tables and Figures

Table 1: Pre-2020 (1998–February 2020): Yield responses to macroeconomic surprises

| | (1) 2-Year | (2) 5-Year | (3) 10-Year |
|---|---|---|---|
| *Panel A: Surprise main effects* | | | |
| Durable | 0.00918*** | 0.0100*** | 0.00747*** |
| | (0.0014) | (0.0016) | (0.0013) |
| GDP (Advance) | 0.0102*** | 0.0141*** | 0.0108*** |
| | (0.0028) | (0.0036) | (0.0029) |
| Core CPI | 0.0129*** | 0.0172*** | 0.0140*** |
| | (0.0018) | (0.0022) | (0.0018) |
| Hourly Earn. | 0.0279*** | 0.0386*** | 0.0310*** |
| | (0.0049) | (0.0063) | (0.0051) |
| Retail ex. auto | 0.0160*** | 0.0190*** | 0.0150*** |
| | (0.0042) | (0.0046) | (0.0036) |
| Unemp. | -0.0338*** | -0.0386*** | -0.0275*** |
| | (0.0069) | (0.0079) | (0.0062) |
| Init. Claims | -0.0291*** | -0.0335*** | -0.0276*** |
| | (0.0027) | (0.0031) | (0.0025) |
| CPI | 0.000539 | 0.00292 | 0.00297* |
| | (0.0017) | (0.0020) | (0.0016) |
| Nonfarm | 0.246*** | 0.290*** | 0.219*** |
| | (0.0231) | (0.0277) | (0.0228) |
| Retail | 0.0101** | 0.0135*** | 0.0107*** |
| | (0.0040) | (0.0044) | (0.0036) |
| *Panel B: Interaction terms (surprise × disagreement)* | | | |
| Init. Claims × $disp^{ICLM}$ | 0.00431 | 0.00752** | 0.00717*** |
| | (0.0030) | (0.0033) | (0.0027) |
| CPI × $disp^{CPI}$ | -0.00226** | -0.00345** | -0.00279** |
| | (0.0010) | (0.0014) | (0.0011) |
| Nonfarm × $disp^{Nonfarm}$ | -0.176*** | -0.260*** | -0.220*** |
| | (0.0594) | (0.0808) | (0.0627) |
| Durable × $disp^{Durable}$ | -0.00483** | -0.00415* | -0.00411** |
| | (0.0023) | (0.0023) | (0.0019) |
| Retail × $disp^{Retail}$ | -0.00318 | -0.00315 | -0.00424 |
| | (0.0049) | (0.0052) | (0.0044) |
| GDP × $disp^{GDP}$ | -0.0247*** | -0.0331*** | -0.0266*** |
| | (0.0093) | (0.0116) | (0.0089) |
| *Panel C: Interaction terms (surprise × short-rate uncertainty)* | | | |
| Init. Claims × $SRU$ | -0.0161*** | -0.0136*** | -0.00832*** |
| | (0.0030) | (0.0036) | (0.0029) |
| CPI × $SRU$ | -0.000246 | -0.00169 | -0.000599 |
| | (0.0017) | (0.0021) | (0.0017) |
| Nonfarm × $SRU$ | 0.0932*** | 0.0710*** | 0.0352* |
| | (0.0209) | (0.0262) | (0.0195) |
| Durable × $SRU$ | 0.00600*** | 0.00524*** | 0.00284* |
| | (0.0017) | (0.0018) | (0.0015) |
| Retail × $SRU$ | 0.0122*** | 0.00968** | 0.00749** |
| | (0.0037) | (0.0039) | (0.0032) |
| GDP × $SRU$ | 0.00707** | 0.00667* | 0.00406 |
| | (0.0030) | (0.0038) | (0.0031) |
| Observations | 2,383 | 2,516 | 2,517 |
| R-squared | 0.425 | 0.406 | 0.380 |

Heteroskedasticity-robust standard errors in parentheses. * $p < 0.10$, ** $p < 0.05$, *** $p < 0.01$. Additional regressors not reported: disagreement levels for each surprise, short-rate uncertainty level, quadratic terms in all surprises and conditioning variables, and controls for VIX, MOVE index, economic policy uncertainty (EPU), Jurado–Ludvigson–Ng macroeconomic uncertainty (JLN), and a zero lower bound dummy. Full results are in Table 7.

Table 2: Post-COVID (July 2020–2024): Yield responses to macroeconomic surprises

| | (1) 2-Year | (2) 5-Year | (3) 10-Year |
|---|---|---|---|
| *Panel A: Surprise main effects* | | | |
| Durable | -0.0106 | -0.00625 | -0.00101 |
| | (0.0105) | (0.0074) | (0.0047) |
| GDP (Advance) | -0.00995 | -0.0120* | -0.0115*** |
| | (0.0142) | (0.0067) | (0.0044) |
| Core CPI | 0.0272*** | 0.0344*** | 0.0250*** |
| | (0.0094) | (0.0094) | (0.0069) |
| Hourly Earn. | 0.0490*** | 0.0450*** | 0.0316*** |
| | (0.0153) | (0.0152) | (0.0117) |
| Retail ex. auto | 0.00413 | 0.00579 | 0.00430 |
| | (0.0076) | (0.0077) | (0.0058) |
| Unemp. | -0.0272** | -0.0295** | -0.0205** |
| | (0.0116) | (0.0121) | (0.0096) |
| Init. Claims | -0.0308 | -0.0414*** | -0.0305*** |
| | (0.0316) | (0.0115) | (0.0075) |
| CPI | 0.0216 | 0.0162 | 0.0104 |
| | (0.0131) | (0.0122) | (0.0088) |
| Nonfarm | 0.191*** | 0.205*** | 0.150*** |
| | (0.0446) | (0.0466) | (0.0388) |
| Retail | -0.0109 | 0.00629 | 0.00595 |
| | (0.0269) | (0.0153) | (0.0109) |
| *Panel B: Interaction terms (surprise × disagreement)* | | | |
| Init. Claims × $disp^{Init.Claims}$ | 0.000619 | 0.000817 | 0.000980** |
| | (0.0009) | (0.0006) | (0.0004) |
| CPI × $disp^{CPI}$ | -0.0335** | -0.0358** | -0.0312*** |
| | (0.0162) | (0.0152) | (0.0107) |
| Nonfarm × $disp^{Nonfarm}$ | -0.0344* | -0.0258 | -0.0160 |
| | (0.0198) | (0.0207) | (0.0171) |
| Durable × $disp^{Durable}$ | 0.00541 | -0.0000503 | -0.00735 |
| | (0.0153) | (0.0116) | (0.0077) |
| Retail × $disp^{Retail}$ | -0.000675 | -0.0116** | -0.00951** |
| | (0.0138) | (0.0053) | (0.0038) |
| GDP × $disp^{GDP}$ | 0.0209 | 0.0143 | 0.0130* |
| | (0.0138) | (0.0102) | (0.0072) |
| *Panel C: Interaction terms (surprise × short-rate uncertainty)* | | | |
| Init. Claims × $SRU$ | -0.0139 | -0.0201*** | -0.0136*** |
| | (0.0191) | (0.0067) | (0.0043) |
| CPI × $SRU$ | 0.0275*** | 0.0306*** | 0.0216*** |
| | (0.0062) | (0.0066) | (0.0053) |
| Nonfarm × $SRU$ | 0.0166 | 0.0244 | 0.0208 |
| | (0.0247) | (0.0251) | (0.0206) |
| Durable × $SRU$ | 0.00666 | 0.000328 | -0.000891 |
| | (0.0058) | (0.0037) | (0.0028) |
| Retail × $SRU$ | -0.00891 | -0.00279 | -0.00201 |
| | (0.0085) | (0.0053) | (0.0038) |
| GDP × $SRU$ | 0.00385 | 0.00510 | 0.00484 |
| | (0.0046) | (0.0049) | (0.0037) |
| Observations | 375 | 375 | 375 |
| R-squared | 0.247 | 0.546 | 0.552 |

Heteroskedasticity-robust standard errors in parentheses. * $p < 0.10$, ** $p < 0.05$, *** $p < 0.01$. Additional regressors not reported: disagreement levels for each surprise, short-rate uncertainty level, quadratic terms in all surprises and conditioning variables, and controls for VIX, MOVE index, economic policy uncertainty (EPU), Jurado–Ludvigson–Ng macroeconomic uncertainty (JLN), and a zero lower bound dummy. Full results are in Table 9.

Table 3: Chow Tests for Structural Break at COVID

| Maturity | $N$ | $\Delta\beta_{\text{SRU}}$ | $F$-statistic | $df_1$ | $df_2$ | $p$-value |
|---|---|---|---|---|---|---|
| *Panel A: CPI-coefficient subset, CPI-release sample* | | | | | | |
| 2-Year | 371 | $0.0298^{***}$ | 61.21 | 3 | 352 | $< 0.001$ |
| 5-Year | 386 | $0.0330^{***}$ | 49.29 | 3 | 367 | $< 0.001$ |
| 10-Year | 386 | $0.0233^{***}$ | 38.26 | 3 | 367 | $< 0.001$ |
| *Panel B: NFP-coefficient subset, NFP-release sample* | | | | | | |
| 2-Year | 363 | $-0.1024^{***}$ | 7.76 | 3 | 343 | $< 0.001$ |
| 5-Year | 366 | $-0.0754^{**}$ | 6.78 | 3 | 346 | $< 0.001$ |
| 10-Year | 365 | -0.0354 | 5.89 | 3 | 345 | $< 0.001$ |
| *Panel C: Full-coefficient Chow test, pooled sample* | | | | | | |
| 2-Year | 2758 | – | 6.67 | 47 | 2664 | $< 0.001$ |
| 5-Year | 2891 | – | 7.39 | 47 | 2797 | $< 0.001$ |
| 10-Year | 2892 | – | 6.44 | 47 | 2798 | $< 0.001$ |

*Notes.* Panel A restricts the sample to CPI-release dates (`cpixfedum` $= 1$) and tests whether the CPI surprise coefficient, its interaction with CPI release disagreement, and its interaction with short rate uncertainty differ across the pre-2020 (1998–February 2020) and post-COVID (July 2020–2024) subsamples. Implementation interacts a post-COVID indicator with those three regressors and $F$-tests their joint significance; $df_1 = 3$ is the number of restrictions. Panel B is the analogous subset test for NFP-related coefficients, restricted to NFP release dates. Panel C is the full coefficient Chow test on the GDP-extended specification (47 parameters including the constant), run on the pooled all-release sample. The column $\Delta\beta_{\text{SRU}}$ reports the point estimate of the shift (pre-to-post change) in the SRU interaction coefficient: i.e., the coefficient on post $\times$ (CPI $\times$ SRU) in Panel A and post $\times$ (NFP $\times$ SRU) in Panel B. Its sign gives the direction of the change; the $F$-test gives the joint significance of all three shifts in that panel. Significance stars on $\Delta\beta_{\text{SRU}}$ are $^{*}p < 0.10$, $^{**}p < 0.05$, $^{***}p < 0.01$. The COVID gap (March–June 2020) is excluded from all tests.

Table 4: Baseline Calibration

| Parameter | Description | Symbol | Value |
|---|---|---|---|
| *State process* | | | |
| Persistence | AR(1) coefficient | $\rho$ | 0.995 |
| Innovation s.d. | State shock volatility | $\sigma_\varepsilon$ | 0.25 |
| *Survey and disagreement* | | | |
| Number of forecasters | | $J$ | 40 |
| Between-model share | Share of $\mathcal{D}$ from heterogeneity | $\lambda$ | 0.40 |
| Model-component s.d. | s.d. of forecaster bias $c_{M_i}$ | $\sigma_c$ | 0.30 |
| Forecast-noise s.d. | s.d. of $\varepsilon_{i,d-1}$ | $\sigma_z$ | 0.25 |
| *Announcement* | | | |
| Announcement noise s.d. | | $\sigma_u$ | 0.10 |
| *Short rate* | | | |
| Short-rate persistence | | $\phi$ | 0.90 |
| Low-regime response | | $\theta_{x,L}$ | 0.20 |
| High-regime response | | $\theta_{x,H}$ | 1.20 |
| Short-rate shock s.d. | | $\sigma_\eta$ | 0.10 |
| *Regime learning* | | | |
| Diagnostic content | Mean shift between regimes | $\Delta\mu$ | 2.0 |
| Initial prior | $P(g_d = H)$ | $p_0$ | 0.50 |
| *Simulation* | | | |
| Announcement days | | $N$ | 5,000 |
| Burn-in | (discarded) | | 200 |
| Yield maturities | | $h$ | 2, 5, 10 yr |

Table 5: SMM Estimation of Time-Varying Signal Precision Parameters

*Panel A: Parameter Estimates*

| Parameter | Symbol | Estimate | s.e. |
|---|---|---|---|
| Policy slope spread, pre-2020 | $\Delta\theta_x^{\text{pre}}$ | 0.0196 | (0.0003) |
| Policy slope spread, post-COVID | $\Delta\theta_x^{\text{post}}$ | 0.0200 | (0.0007) |
| NFP regime mean shift, pre-2020 | $\Delta\mu_{\text{pre}}^{\text{nfp}}$ | 0.8860 | (0.0033) |
| NFP regime mean shift, post-COVID | $\Delta\mu_{\text{post}}^{\text{nfp}}$ | 0.5743 | (0.0059) |
| CPI regime mean shift, pre-2020 | $\Delta\mu_{\text{pre}}^{\text{cpi}}$ | 0.0054 | (0.0067) |
| CPI regime mean shift, post-COVID | $\Delta\mu_{\text{post}}^{\text{cpi}}$ | 1.5511 | (0.0363) |

*Panel B: Specification Tests*

| Test | Statistic | df | $p$-value |
|---|---|---|---|
| SMM $J$-statistic | 52556.6082 | 18 | 0.0000 |
| LR test of $\Delta\theta_x^{\text{pre}} = \Delta\theta_x^{\text{post}}$ | -31.6216 | 1 | 1.0000 |
| Wald test of $\Delta\theta_x^{\text{pre}} = \Delta\theta_x^{\text{post}}$ | 0.4028 | 1 | 0.5257 |

*Panel C: Targeted vs Fitted Moments by Maturity*

| | | 2-year | | 5-year | | 10-year | |
|---|---|---|---|---|---|---|---|
| Block | Coefficient | Target | Model | Target | Model | Target | Model |
| NFP pre-2020 | $\hat{\beta}_1^{\text{NFP}}$ | 0.2460 | 0.4062*** | 0.2900 | 0.1769*** | 0.2190 | 0.0900*** |
| | | | (6.42) | | (-3.78) | | (-5.24) |
| | $\hat{\beta}_5^{\text{NFP}}$ | 0.0932 | 0.1069 | 0.0710 | 0.0465 | 0.0352 | 0.0234 |
| | | | (0.60) | | (-0.86) | | (-0.56) |
| NFP post-COVID | $\hat{\beta}_1^{\text{NFP}}$ | 0.1910 | 0.2448 | 0.2050 | 0.1066* | 0.1500 | 0.0536** |
| | | | (1.12) | | (-1.95) | | (-2.30) |
| | $\hat{\beta}_5^{\text{NFP}}$ | 0.0166 | 0.0219 | 0.0244 | 0.0096 | 0.0208 | 0.0048 |
| | | | (0.20) | | (-0.55) | | (-0.72) |
| CPI pre-2020 | $\hat{\beta}_1^{\text{CPI}}$ | 0.0005 | 0.0224*** | 0.0029 | 0.0098*** | 0.0030 | 0.0049 |
| | | | (11.91) | | (3.17) | | (1.12) |
| | $\hat{\beta}_5^{\text{CPI}}$ | -0.0002 | 0.0004 | -0.0017 | 0.0002 | -0.0006 | 0.0001 |
| | | | (0.34) | | (0.82) | | (0.37) |
| CPI post-COVID | $\hat{\beta}_1^{\text{CPI}}$ | 0.0216 | 0.0389 | 0.0162 | 0.0169 | 0.0104 | 0.0086 |
| | | | (1.22) | | (0.06) | | (-0.19) |
| | $\hat{\beta}_5^{\text{CPI}}$ | 0.0275 | 0.0152* | 0.0306 | 0.0066*** | 0.0216 | 0.0033*** |
| | | | (-1.84) | | (-3.36) | | (-3.19) |

*Notes.* Joint SMM estimation of six structural parameters across four release-period blocks (NFP and CPI, pre-2020 and post-COVID) at three maturities (2-, 5-, and 10-year). Targeted moments are the main-surprise coefficient $\hat{\beta}_1$ and the surprise×SRU interaction coefficient $\hat{\beta}_5$ from Tables 1 and 2, giving 24 target moments and 18 over-identifying restrictions. Announcement-noise standard deviations $\sigma_u^{\text{nfp}}$ and $\sigma_u^{\text{cpi}}$ are held at calibrated values across periods. Standard errors in Panel A are asymptotic SMM standard errors based on the sandwich formula $\text{Var}(\hat{\theta}) = (1 + 1/\tau)(G'WG)^{-1}\, G'W\Omega WG\, (G'WG)^{-1}/n_{\text{emp}}$, with $G$ the Jacobian of model moments at $\hat{\theta}$, $\Omega$ the empirical variance-covariance matrix of the targeted regression coefficients, $\tau = N_{\text{sim}}/n_{\text{emp}}$, and $n_{\text{emp}} \approx 840$ release dates. The SMM objective uses scale-invariant weighting $W = \text{diag}(1/\max(|\hat{\beta}|, 0.01)^2)$. The LR test compares the unrestricted and the constrained ($\Delta\theta_x^{\text{pre}} = \Delta\theta_x^{\text{post}}$) values of the SMM objective. The $J$-statistic is inflated by the 18 over-identifying restrictions and small per-moment discrepancies; the economically informative diagnostics are the parameter-restriction tests in Panel B and the moment-by-moment fits in Panel C. In Panel C, numbers in parentheses below the model-implied moment are two-sided $t$-statistics for the null that the model-implied moment equals the empirical target, computed as $(m_k^{\text{model}} - \hat{\beta}_k^{\text{data}})/[\sigma_k\sqrt{1 + 1/\tau}]$, where $\sigma_k$ is the empirical regression standard error of the corresponding moment; significance stars use the two-sided $\mathcal{N}(0,1)$ reference ($^{*}$ $p < 0.10$, $^{**}$ $p < 0.05$, $^{***}$ $p < 0.01$). The family-wise 5% Bonferroni critical value across the 24 moment tests is $|t| > 3.08$.

Table 6: Placebo Test: Permutation Null Distribution of Interaction Coefficients

| | Pre-2020 | | | Post-COVID | | |
|---|---|---|---|---|---|---|
| Surprise | 2-Year | 5-Year | 10-Year | 2-Year | 5-Year | 10-Year |
| *Panel A: Surprise × Disagreement ($\hat{\beta}_3$)* | | | | | | |
| CPI | -0.0023 / -0.0001 / 0.144 | -0.0035 / -0.0001 / 0.113 | -0.0028 / -0.0001 / 0.114 | -0.0335 / 0.0001 / 0.076 | -0.0358 / 0.0002 / 0.068 | -0.0312 / 0.0001 / 0.024 |
| NFP | -0.1761 / -0.0014 / 0.002 | -0.2601 / -0.0039 / 0.001 | -0.2205 / -0.0045 / 0.000 | -0.0344 / -0.0252 / 0.593 | -0.0258 / -0.0255 / 0.689 | -0.0160 / -0.0172 / 0.747 |
| Initial Claims | 0.0043 / -0.0003 / 0.424 | 0.0075 / -0.0005 / 0.244 | 0.0072 / -0.0004 / 0.193 | 0.0006 / 0.0015 / 0.928 | 0.0008 / 0.0009 / 0.874 | 0.0010 / 0.0008 / 0.803 |
| Durable Goods | -0.0048 / 0.0000 / 0.060 | -0.0042 / -0.0000 / 0.160 | -0.0041 / -0.0000 / 0.083 | 0.0054 / 0.0005 / 0.601 | -0.0001 / 0.0001 / 0.998 | -0.0073 / 0.0001 / 0.141 |
| Retail Sales | -0.0032 / 0.0003 / 0.768 | -0.0032 / 0.0002 / 0.769 | -0.0042 / 0.0001 / 0.630 | -0.0007 / 0.0007 / 0.970 | -0.0116 / 0.0009 / 0.428 | -0.0095 / 0.0007 / 0.393 |
| GDP | -0.0247 / -0.0001 / 0.105 | -0.0331 / -0.0001 / 0.079 | -0.0266 / -0.0002 / 0.073 | 0.0209 / -0.0010 / 0.179 | 0.0143 / -0.0007 / 0.209 | 0.0130 / -0.0006 / 0.154 |
| *Panel B: Surprise × Short-Rate Uncertainty ($\hat{\beta}_5$)* | | | | | | |
| CPI | -0.0002 / 0.0000 / 0.890 | -0.0017 / 0.0000 / 0.362 | -0.0006 / 0.0000 / 0.677 | 0.0275 / -0.0006 / 0.003 | 0.0306 / -0.0006 / 0.000 | 0.0216 / -0.0004 / 0.001 |
| NFP | 0.0932 / -0.0063 / 0.000 | 0.0710 / -0.0049 / 0.018 | 0.0352 / -0.0025 / 0.102 | 0.0166 / -0.0421 / 0.817 | 0.0244 / -0.0437 / 0.734 | 0.0208 / -0.0320 / 0.697 |
| Initial Claims | -0.0161 / 0.0003 / 0.000 | -0.0136 / 0.0002 / 0.000 | -0.0083 / 0.0002 / 0.000 | -0.0139 / 0.0027 / 0.376 | -0.0201 / 0.0017 / 0.035 | -0.0136 / 0.0017 / 0.057 |
| Durable Goods | 0.0060 / 0.0001 / 0.000 | 0.0052 / 0.0000 / 0.003 | 0.0028 / 0.0000 / 0.055 | 0.0067 / 0.0002 / 0.132 | 0.0003 / 0.0001 / 0.894 | -0.0009 / 0.0000 / 0.621 |
| Retail Sales | 0.0122 / 0.0001 / 0.000 | 0.0097 / 0.0001 / 0.003 | 0.0075 / 0.0001 / 0.005 | -0.0089 / 0.0010 / 0.442 | -0.0028 / 0.0009 / 0.726 | -0.0020 / 0.0007 / 0.734 |
| GDP | 0.0071 / -0.0001 / 0.164 | 0.0067 / -0.0001 / 0.255 | 0.0041 / -0.0001 / 0.365 | 0.0039 / -0.0004 / 0.754 | 0.0051 / -0.0002 / 0.687 | 0.0048 / -0.0001 / 0.612 |

*Notes.* Each cell reports three numbers separated by slashes: the actual interaction coefficient from the announcement-window regression of equation (1), the mean of the permutation null distribution (1000 permutations of surprise values across release dates within each release type), and the two-sided permutation $p$-value. Under the null that the coefficients are spurious products of persistent regime correlations, permuted-surprise estimates should be centered at zero and $p$-values should be uniform on $[0, 1]$.

Figure 1: Marginal Effects of Short-Rate Uncertainty and Survey Disagreement on 2-Year Treasury Futures Responses to Macro Announcements, Pre-2020 Subsample (1998–February 2020)

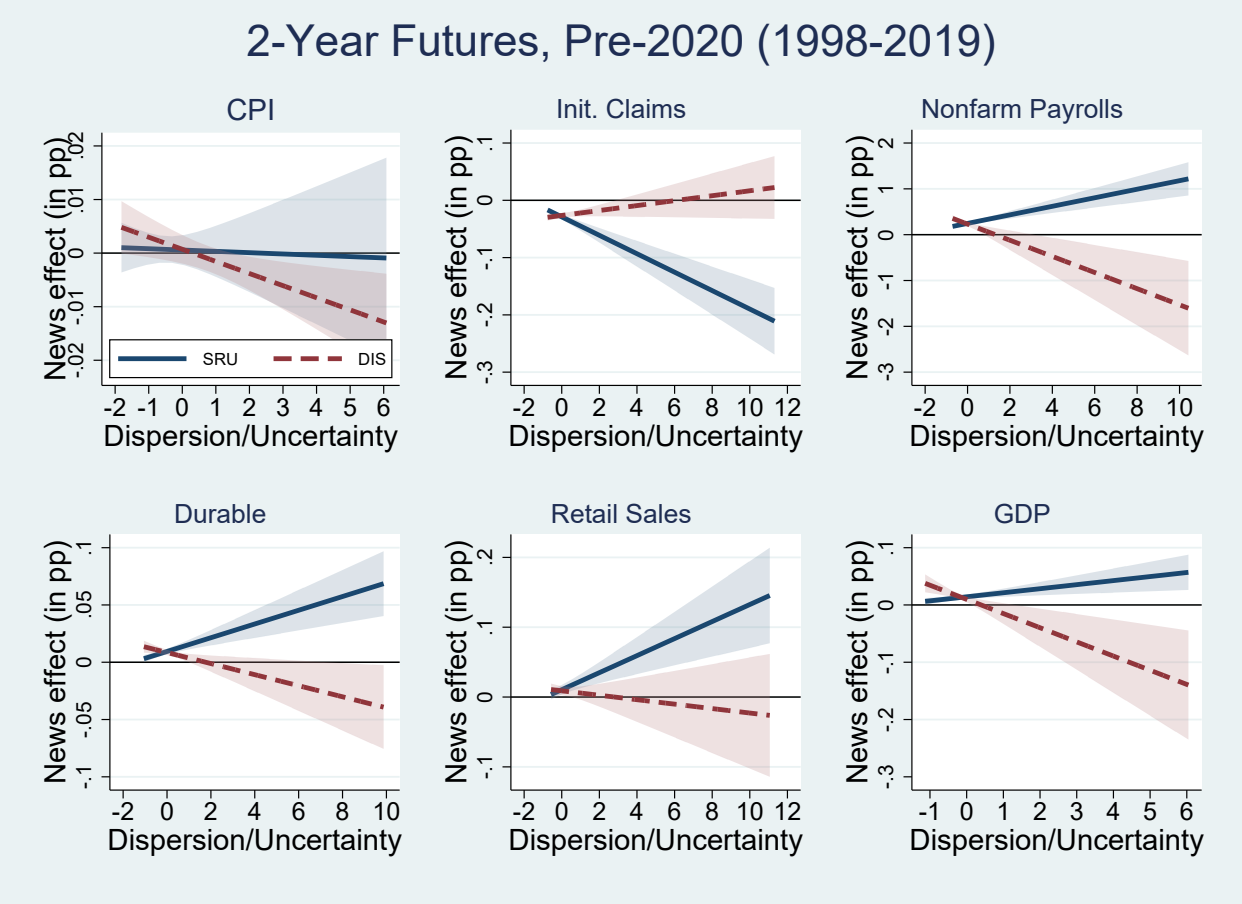


**Note:** Response of 2-year Treasury futures to CPI, initial claims, nonfarm payrolls, durable goods orders, retail sales, and GDP surprises when short rate uncertainty and disagreement are varied. The y-axis measures the marginal effect on the yield change in percentage points per one-standard-deviation surprise. The x-axis represents the level of short-rate uncertainty or survey disagreement in standard deviations relative to the sample mean. The dashed line shows the effects of varied survey disagreement, keeping short rate uncertainty fixed, and the solid line shows the impact of short rate uncertainty when survey disagreement is fixed. Shaded regions show 90% confidence intervals based on heteroskedasticity-robust standard errors. The sample is from 1998 to 2019.

Figure 2: Marginal Effects of Short-Rate Uncertainty and Survey Disagreement on 5-Year Treasury Futures Responses to Macro Announcements, Pre-2020 Subsample (1998–February 2020)

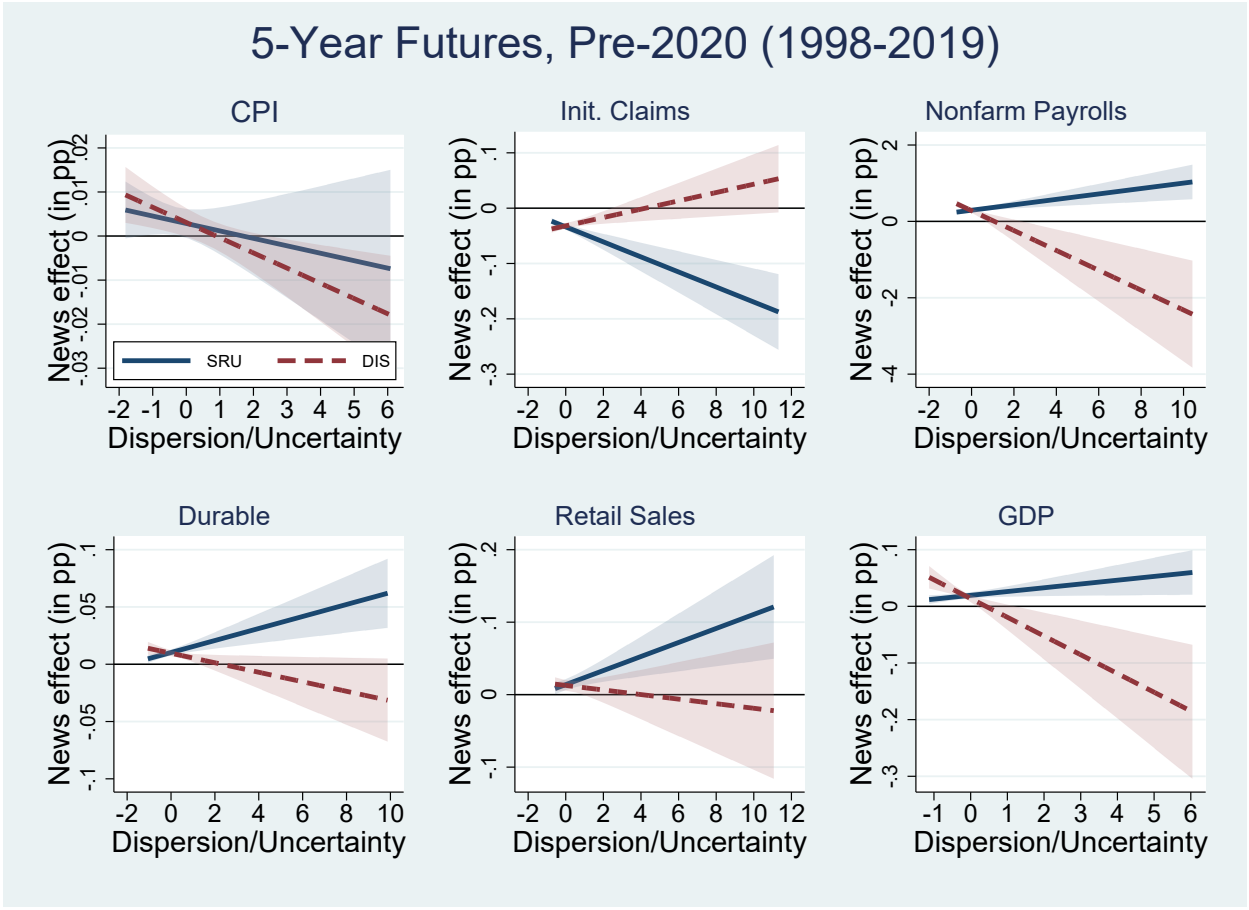


**Note:** Response of 5-year Treasury futures to CPI, initial claims, nonfarm payrolls, durable goods orders, retail sales, and GDP surprises when short rate uncertainty and disagreement are varied. The y-axis measures the marginal effect on the yield change in percentage points per one-standard-deviation surprise. The x-axis represents the level of short-rate uncertainty or survey disagreement in standard deviations relative to the sample mean. The dashed line shows the effects of varied survey disagreement, keeping short rate uncertainty fixed, and the solid line shows the impact of short rate uncertainty when survey disagreement is fixed. Shaded regions show 90% confidence intervals based on heteroskedasticity-robust standard errors. The sample is from 1998 to 2019.

Figure 3: Marginal Effects of Short-Rate Uncertainty and Survey Disagreement on 10-Year Treasury Futures Responses to Macro Announcements, Pre-2020 Subsample (1998–February 2020)

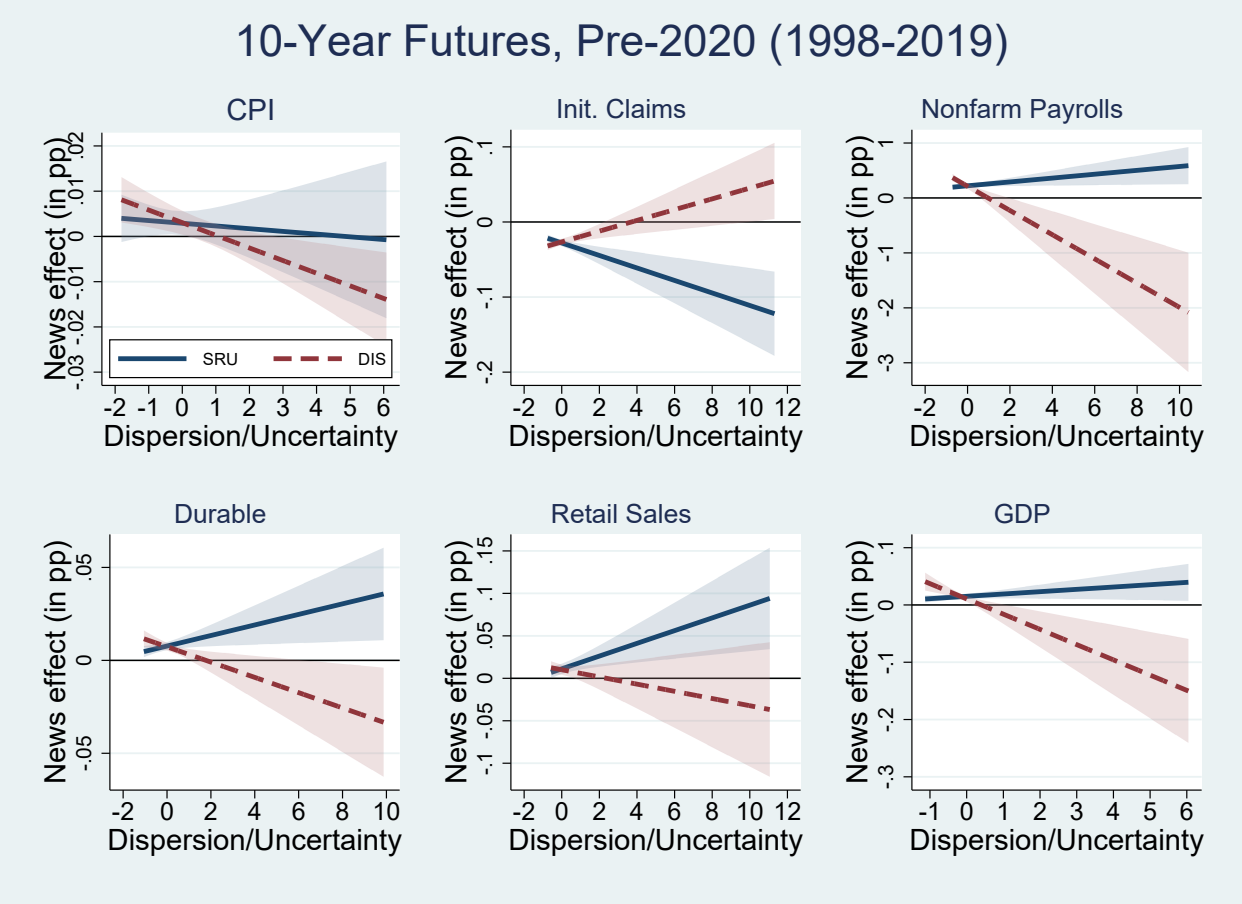


**Note:** Response of 10-year Treasury futures to CPI, initial claims, nonfarm payrolls, durable goods orders, retail sales, and GDP surprises when short rate uncertainty and disagreement are varied. The y-axis measures the marginal effect on the yield change in percentage points per one-standard-deviation surprise. The x-axis represents the level of short-rate uncertainty or survey disagreement in standard deviations relative to the sample mean. The dashed line shows the effects of varied survey disagreement, keeping short rate uncertainty fixed, and the solid line shows the impact of short rate uncertainty when survey disagreement is fixed. Shaded regions show 90% confidence intervals based on heteroskedasticity-robust standard errors. The sample is from 1998 to 2019.

Figure 4: Marginal Effects of Short-Rate Uncertainty and Survey Disagreement on 2-Year Treasury Futures Responses to Macro Announcements, Post-COVID Subsample (July 2020–2024)

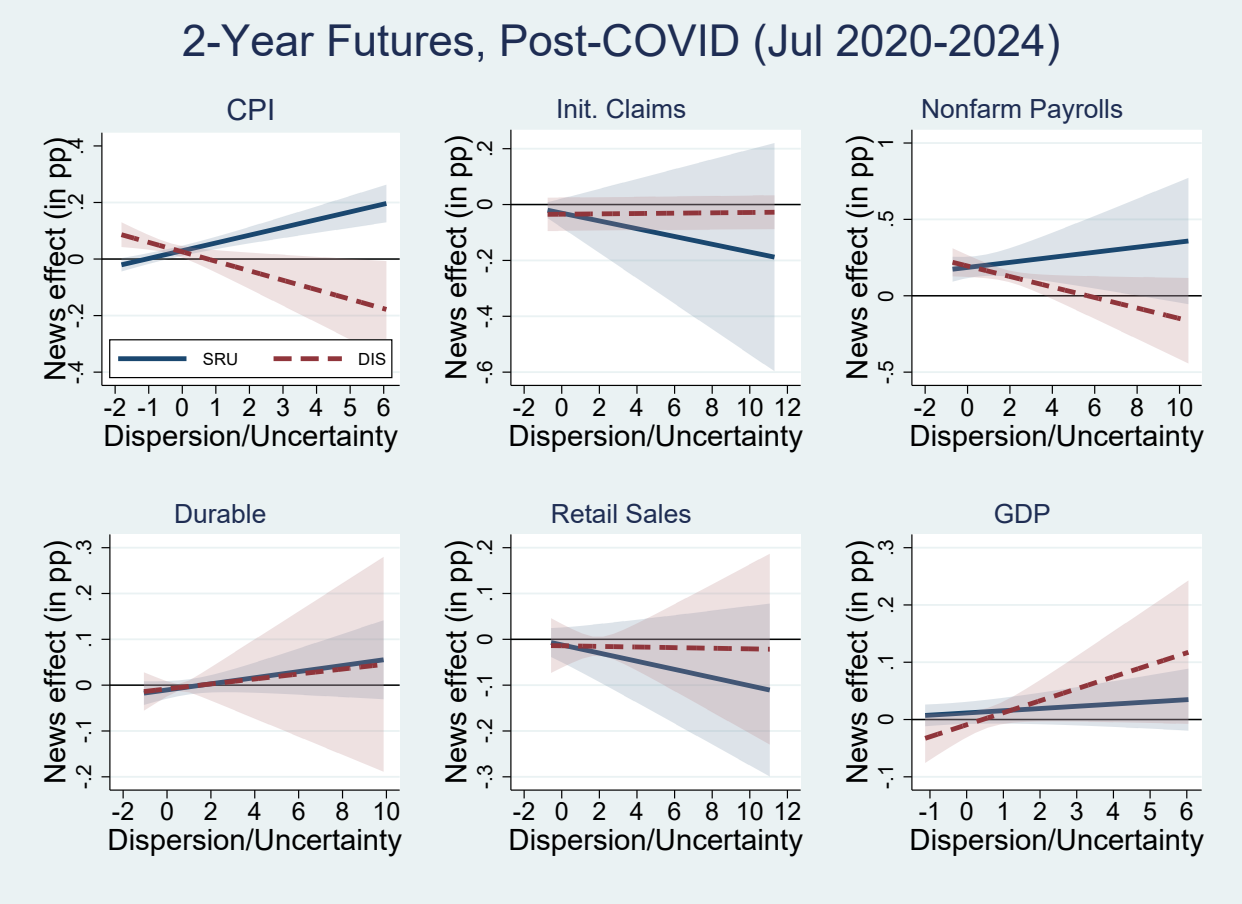


**Note:** Response of 2-year Treasury futures to CPI, initial claims, nonfarm payrolls, durable goods orders, retail sales, and GDP surprises when short rate uncertainty and disagreement are varied. The y-axis measures the marginal effect on the yield change in percentage points per one-standard-deviation surprise. The x-axis represents the level of short-rate uncertainty or survey disagreement in standard deviations relative to the sample mean. The dashed line shows the effects of varied survey disagreement, keeping short rate uncertainty fixed, and the solid line shows the impact of short rate uncertainty when survey disagreement is fixed. Shaded regions show 90% confidence intervals based on heteroskedasticity-robust standard errors. The sample is from July 2020 to 2024.

Figure 5: Marginal Effects of Short-Rate Uncertainty and Survey Disagreement on 5-Year Treasury Futures Responses to Macro Announcements, Post-COVID Subsample (July 2020–2024)

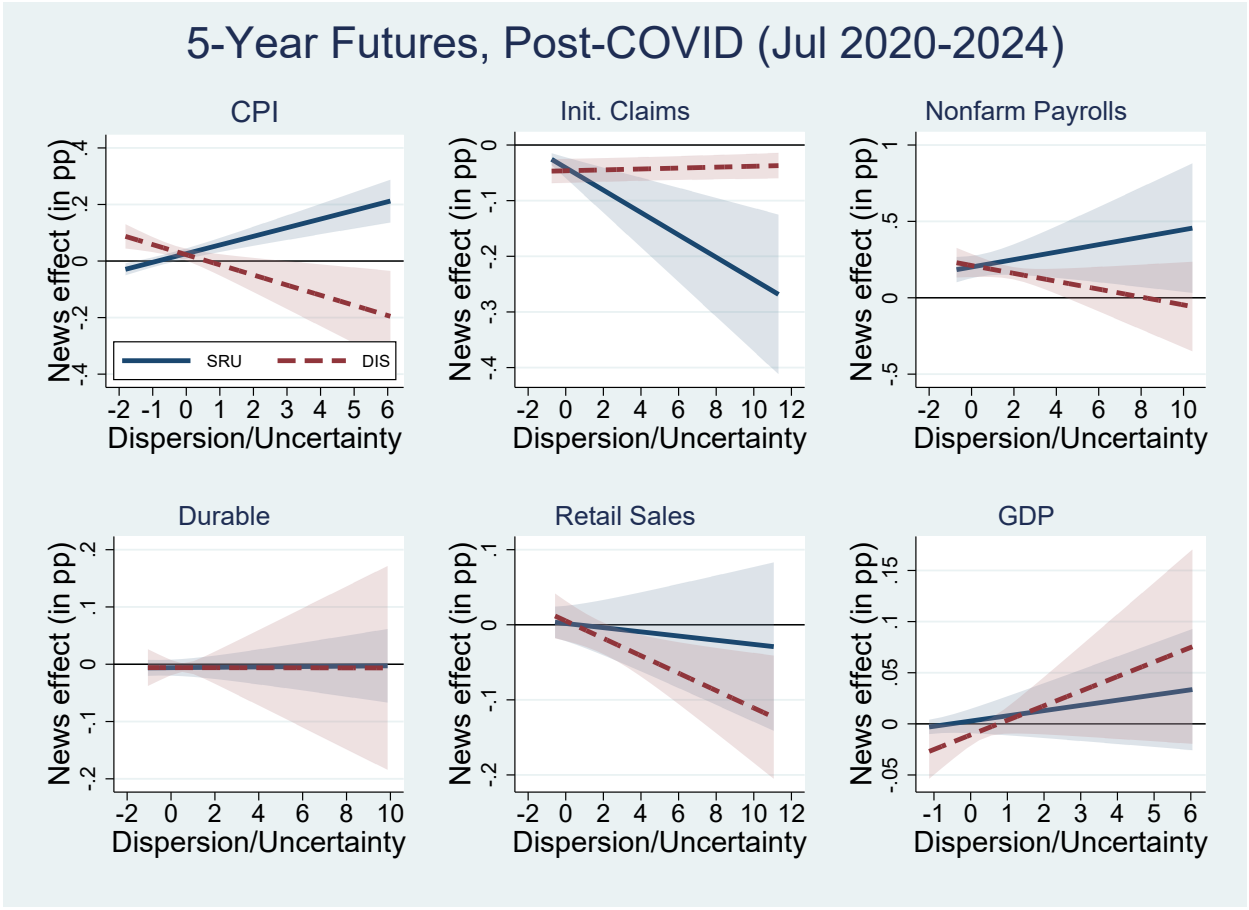


**Note:** Response of 5-year Treasury futures to CPI, initial claims, nonfarm payrolls, durable goods orders, retail sales, and GDP surprises when short rate uncertainty and disagreement are varied. The y-axis measures the marginal effect on the yield change in percentage points per one-standard-deviation surprise. The x-axis represents the level of short-rate uncertainty or survey disagreement in standard deviations relative to the sample mean. The dashed line shows the effects of varied survey disagreement, keeping short rate uncertainty fixed, and the solid line shows the impact of short rate uncertainty when survey disagreement is fixed. Shaded regions show 90% confidence intervals based on heteroskedasticity-robust standard errors. The sample is from July 2020 to 2024.

Figure 6: Marginal Effects of Short-Rate Uncertainty and Survey Disagreement on 10-Year Treasury Futures Responses to Macro Announcements, Post-COVID Subsample (July 2020–2024)

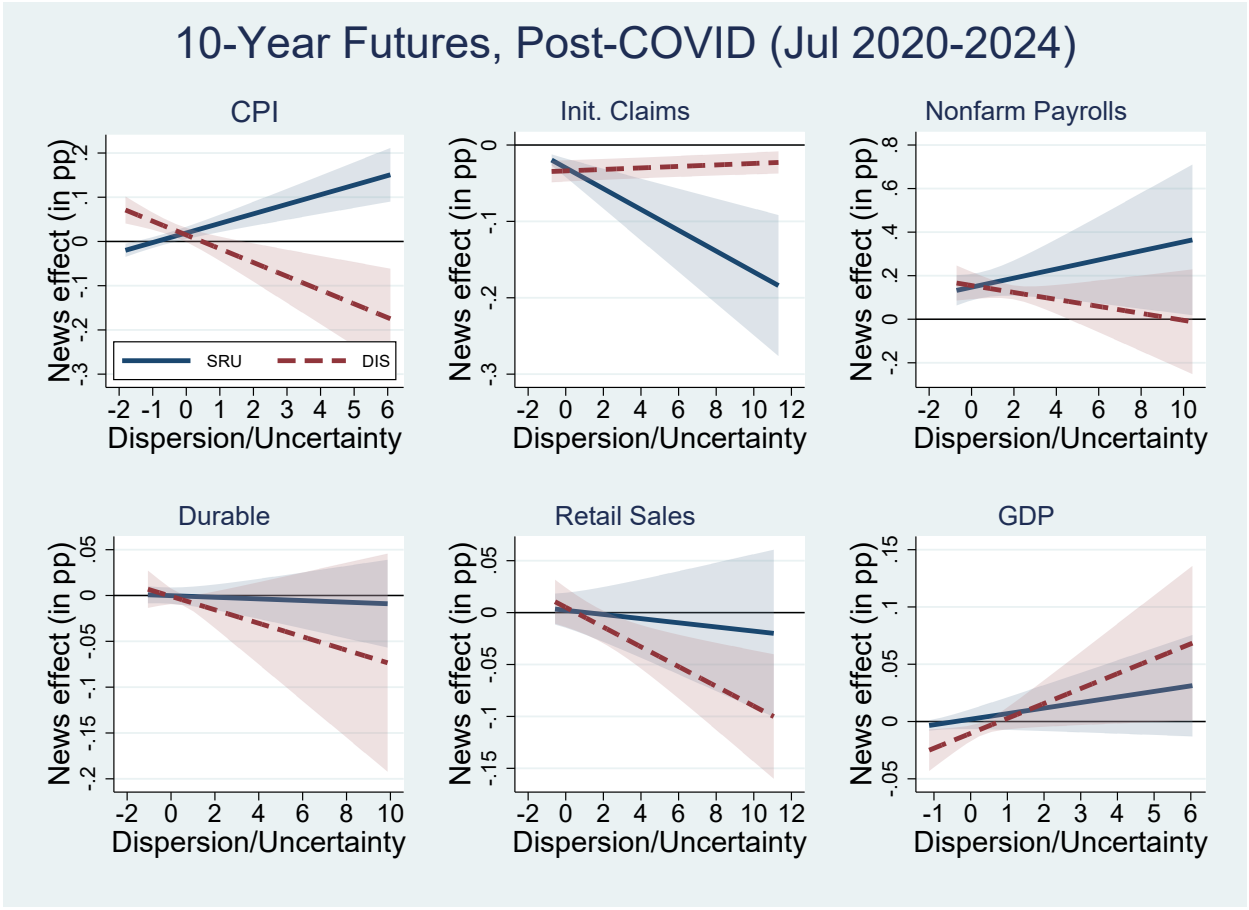


**Note:** Response of 10-year Treasury futures to CPI, initial claims, nonfarm payrolls, durable goods orders, retail sales, and GDP surprises when short rate uncertainty and disagreement are varied. The y-axis measures the marginal effect on the yield change in percentage points per one-standard-deviation surprise. The x-axis represents the level of short-rate uncertainty or survey disagreement in standard deviations relative to the sample mean. The dashed line shows the effects of varied survey disagreement, keeping short rate uncertainty fixed, and the solid line shows the impact of short rate uncertainty when survey disagreement is fixed. Shaded regions show 90% confidence intervals based on heteroskedasticity-robust standard errors. The sample is from July 2020 to 2024.

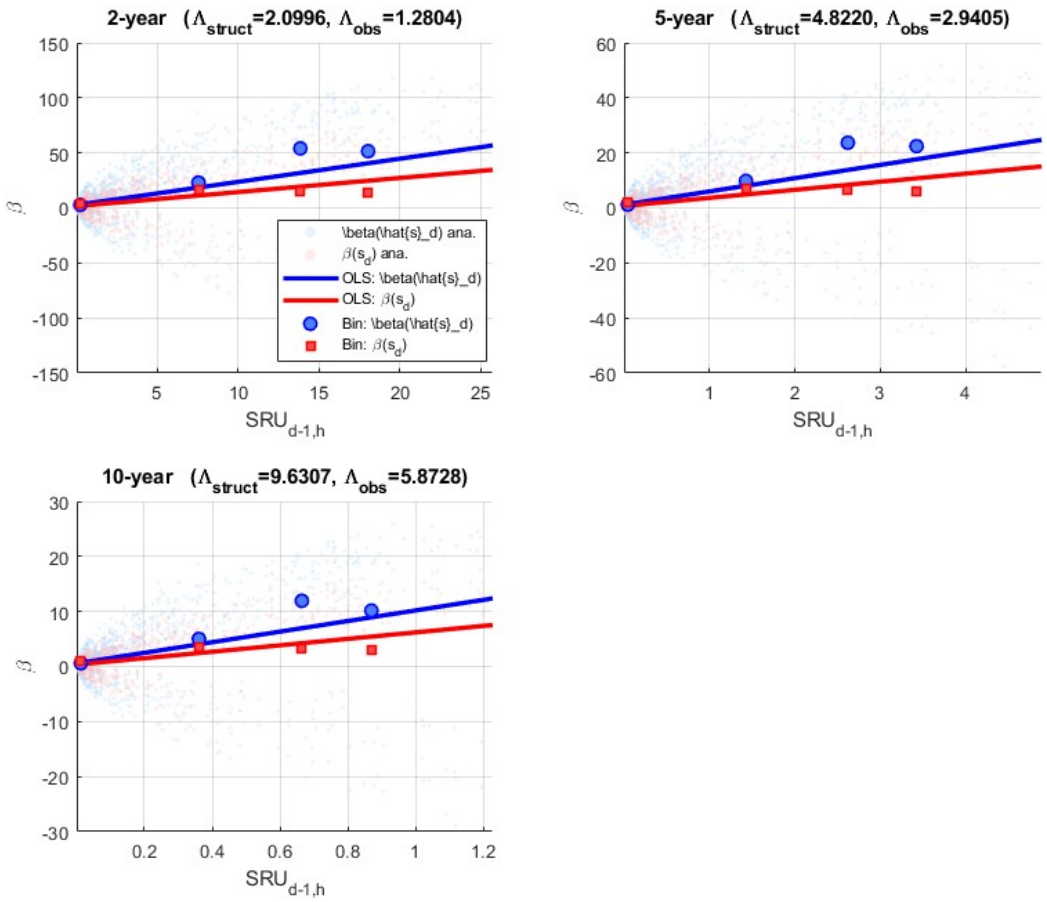


Figure 7: Yield-response coefficient vs. short-rate uncertainty. Each panel corresponds to a maturity (2, 5, and 10 years). Light dots show observation level analytical $\beta$ values; solid lines are OLS fits through the analytical scatter; circles and squares are binned estimates from simulated yield data.

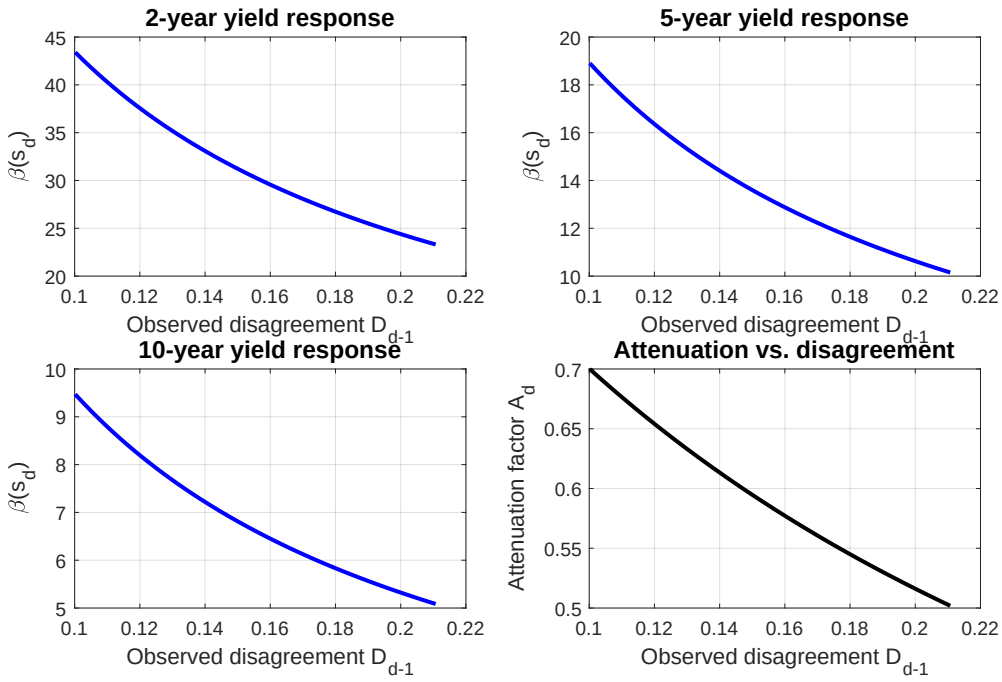


Figure 8: Effect of forecast disagreement on the observed-surprise coefficient $\beta_h(s_d)$ at 2-, 5-, and 10-year maturities (top left, top right, bottom left). Bottom right panel shows the attenuation factor $\mathcal{A}_d$. All curves are computed at median values of the remaining state variables.

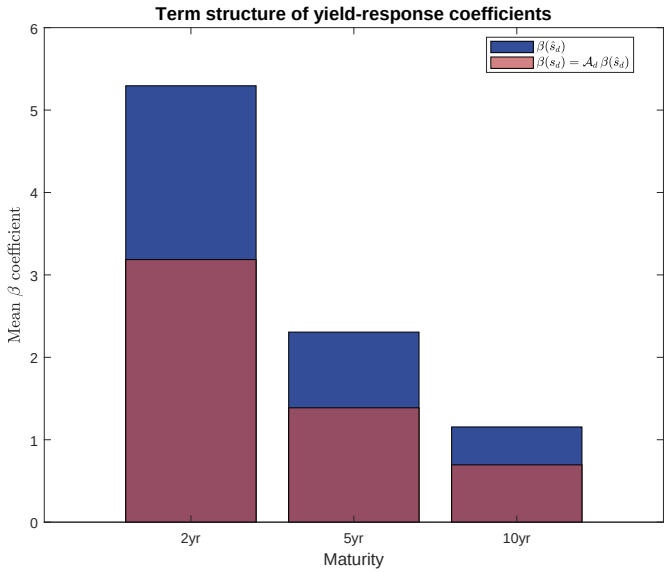


Figure 9: Average yield response coefficients across maturities. Dark bars: structural-surprise coefficient $\bar{\beta}_h(\hat{s}_d)$. Light bars: observed-surprise coefficient $\bar{\beta}_h(s_d) = \bar{\mathcal{A}}_d \cdot \bar{\beta}_h(\hat{s}_d)$.

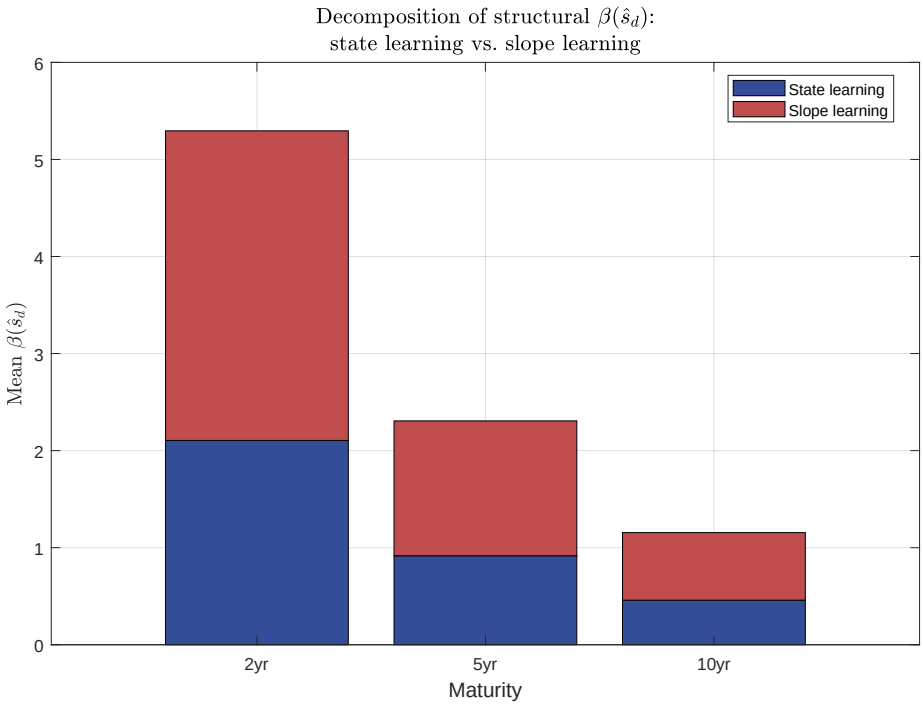


Figure 10: Decomposition of the average structural surprise coefficient into state learning and slope learning across maturities.

## References


Altavilla, Carlo, Domenico Giannone, and Michele Modugno (2017). "Low frequency effects of macroeconomic news on government bond yields". In: *Journal of Monetary Economics* 92, pp. 31–46.

Andersen, Torben G, Tim Bollerslev, Francis X Diebold, and Clara Vega (2007). "Real-time price discovery in global stock, bond and foreign exchange markets". In: *Journal of international Economics* 73.2, pp. 251–277.

Baker, Scott R, Nicholas Bloom, and Steven J Davis (2016). "Measuring economic policy uncertainty". In: *The Quarterly Journal of Economics* 131.4, pp. 1593–1636.

Balduzzi, Pierluigi, Edwin J Elton, and T Clifton Green (2001). "Economic news and bond prices: Evidence from the US Treasury market". In: *Journal of financial and Quantitative analysis* 36.4, pp. 523–543.

Barbera, Alessandro, Fan Dora Xia, and Xingyu Zhu (2023). "The term structure of inflation forecasts disagreement and monetary policy transmission". In: *BIS Working Papers*.

Bauer, Michael D, Aeimit Lakdawala, and Philippe Mueller (2022). "Market-based monetary policy uncertainty". In: *The Economic Journal* 132.644, pp. 1290–1308.

Bauer, Michael D, Carolin Pflueger, and Adi Sunderam (2025). "Current Perceptions About Monetary Policy". In: *FRBSF Economic Letter* 2025.05, pp. 1–6.

Beber, Alessandro and Michael W Brandt (2010). "When it cannot get better or worse: The asymmetric impact of good and bad news on bond returns in expansions and recessions". In: *Review of Finance* 14.1, pp. 119–155.

Bernanke, Ben S and Kenneth N Kuttner (2005). "What explains the stock market's reaction to Federal Reserve policy?" In: *The Journal of Finance* 60.3, pp. 1221–1257.

Born, Benjamin, Jonas Dovern, and Zeno Enders (2023). "Expectation dispersion, uncertainty, and the reaction to news". In: *European Economic Review* 154, p. 104440.

Boyd, John H, Jian Hu, and Ravi Jagannathan (2005). "The stock market's reaction to unemployment news: Why bad news is usually good for stocks". In: *The Journal of Finance* 60.2, pp. 649–672.

Cieslak, Anna and Hao Pang (2021). "Common shocks in stocks and bonds". In: *Journal of Financial Economics* 142.2, pp. 880–904.

Coibion, Olivier and Yuriy Gorodnichenko (2012). "What can survey forecasts tell us about information rigidities?" In: *Journal of Political Economy* 120.1, pp. 116–159.

Coibion, Olivier and Yuriy Gorodnichenko (2015). "Information rigidity and the expectations formation process: A simple framework and new facts". In: *American Economic Review* 105.8, pp. 2644–2678.

Faust, Jon, John H Rogers, Shing-Yi B Wang, and Jonathan H Wright (2007). "The high-frequency response of exchange rates and interest rates to macroeconomic announcements". In: *Journal of Monetary Economics* 54.4, pp. 1051–1068.

Fleming, Michael J and Eli M Remolona (1997). "What moves the bond market?" In: *Economic policy review* 3.4.

Goldberg, Linda S and Christian Grisse (2013). "Time variation in asset price responses to macro announcements". In: *NBER Working Papers*.

Gürkaynak, Refet S, Burçin Kısacıkoğlu, and Jonathan H Wright (2020). "Missing events in event studies: Identifying the effects of partially measured news surprises". In: *American Economic Review* 110.12, pp. 3871–3912.

Gürkaynak, Refet S, Brian Sack, and Eric Swanson (2005). "The sensitivity of long-term interest rates to economic news: Evidence and implications for macroeconomic models". In: *American economic review* 95.1, pp. 425–436.

Hirshleifer, David and Jinfei Sheng (2022). "Macro news and micro news: complements or substitutes?" In: *Journal of Financial Economics* 145.3, pp. 1006–1024.

Hobijn, Bart and Ayşegül Şahin (2023). *Missing Workers and Missing Jobs Since the Pandemic*. NBER Working Paper 30717. National Bureau of Economic Research.

Hördahl, Peter, Eli M Remolona, and Giorgio Valente (2020). "Expectations and risk premia at 8: 30 am: Deciphering the responses of bond yields to macroeconomic announcements". In: *Journal of Business & Economic Statistics* 38.1, pp. 27–42.

Kandel, Eugine and Neil D Pearson (1995). "Differential interpretation of public signals and trade in speculative markets". In: *Journal of Political Economy* 103, pp. 831–872.

Kroner, T Niklas (2025). "How Markets Process Macro News: The Importance of Investor Attention". In: *Finance and Economics Discussion Series*.

Kuttner, Kenneth N (2001). "Monetary policy surprises and interest rates: Evidence from the Fed funds futures market". In: *Journal of Monetary Economics* 47.3, pp. 523–544.

Leduc, Sylvain, Luiz Edgard Oliveira, and Caroline Paulson (2025). "Do Low Survey Response Rates Threaten Data Dependence?" In: *FRBSF Economic Letter* 2025.07.

Logan, Lorie (2020). *Treasury market liquidity and early lessons from the pandemic shock*. Remarks at Brookings-Chicago Booth Task Force on Financial Stability Meeting.

Maćkowiak, Bartosz and Mirko Wiederholt (2009). "Optimal sticky prices under rational inattention". In: *American Economic Review* 99.3, pp. 769–803.

Mankiw, N Gregory, Ricardo Reis, and Justin Wolfers (2004). "Disagreement about inflation expectations". In: *NBER Macroeconomics Annual* 18, pp. 209–248.

Merton, Robert C (1969). "Lifetime portfolio selection under uncertainty: the continuous-time case". In: *Review of Economics and Statistics* 51, pp. 247–257.

Nakamura, Emi and Jón Steinsson (2018). "High-frequency identification of monetary non-neutrality: The information effect". In: *The Quarterly Journal of Economics* 133.3, pp. 1283–1330.

Patton, Andrew J and Allan Timmermann (2010). "Why do forecasters disagree? Lessons from the term structure of cross-sectional dispersion". In: *Journal of Monetary Economics* 57.7, pp. 803–820.

Pericoli, Marcello and Giovanni Veronese (2015). "Forecaster heterogeneity, surprises and financial markets". In: *Bank of Italy Temi di Discussione (Working paper) No* 1020.

Pfäuti, Oliver (2026). "The Inflation Attention Threshold and Inflation Surges". In: *University of Texas at Austin Working Paper*.

Sims, Christopher A (2003). "Implications of rational inattention". In: *Journal of Monetary Economics* 50.3, pp. 665–690.

Swanson, Eric T and John C Williams (2014). "Measuring the effect of the zero lower bound on medium-and longer-term interest rates". In: *American economic review* 104.10, pp. 3154–3185.

Woodford, Michael (2003). "Imperfect common knowledge and the effects of monetary policy". In: *Knowledge, Information, and Expectations in Modern Macroeconomics: In Honor of Edmund S. Phelps*. Ed. by Philippe Aghion, Roman Frydman, Joseph Stiglitz, and Michael Woodford. Princeton University Press, pp. 25–58.

Xia, Fan Dora and Xingyu Sonya Zhu (2025). "Macroeconomic news and repricing of monetary policy expectations". In: *Economics Letters*, p. 112779.

# Appendix A Model Derivations

This appendix collects the detailed derivations of the model equations stated in Section 5. Each subsection below corresponds to a main text subsection and supplies the algebra that was summarized there.

## A.1 Day $d-1$: Consensus Decomposition and Effective Variance

**Decomposition of the consensus.** Substituting $z_{i,d-1} = x_d + c_{M_{i,d-1}} + \varepsilon_{i,d-1}$ into $m_{d-1} = J^{-1}\sum_i z_{i,d-1}$ gives $m_{d-1} = x_d + \bar{c}_{d-1} + \bar{\varepsilon}_{d-1}$, where $\bar{c}_{d-1} = J^{-1}\sum_i c_{M_{i,d-1}}$ and $\bar{\varepsilon}_{d-1} = J^{-1}\sum_i \varepsilon_{i,d-1}$. Because the individual noise terms are iid across forecasters with variance $\sigma^2_{\varepsilon,d-1}$,

$$\mathrm{Var}(\bar{\varepsilon}_{d-1} \mid \mathcal{F}_{d-1}) = \sigma^2_{\varepsilon,d-1}/J.$$

The between-model component $\bar{c}_{d-1}$ is *not* iid across forecasters (forecasters sharing the same model $M_i$ share the same draw of $c_{M_i}$), so its variance $\Omega_{d-1} \equiv \mathrm{Var}(\bar{c}_{d-1} \mid \mathcal{F}_{d-1})$ does not shrink at rate $1/J$.

**Observed disagreement.** By construction $\mathcal{D}_{d-1} = J^{-1}\sum_i (z_{i,d-1} - m_{d-1})^2$. Using the identity $z_{i,d-1} - m_{d-1} = (c_{M_{i,d-1}} - \bar{c}_{d-1}) + (\varepsilon_{i,d-1} - \bar{\varepsilon}_{d-1})$, squaring and averaging,

$$\mathcal{D}_{d-1} = \underbrace{\tfrac{1}{J}\sum_i (c_{M_{i,d-1}} - \bar{c}_{d-1})^2}_{B_{d-1}} + \tfrac{1}{J}\sum_i (\varepsilon_{i,d-1} - \bar{\varepsilon}_{d-1})^2 + \text{cross term}.$$

Taking conditional expectations and using the orthogonality of model assignment and within model noise, the cross term drops out, yielding $\mathrm{E}[\mathcal{D}_{d-1} \mid \mathcal{F}_{d-1}] = B_{d-1} + \sigma^2_{\varepsilon,d-1}$.

**Effective consensus error variance.** The consensus error is $m_{d-1} - x_d = \bar{c}_{d-1} + \bar{\varepsilon}_{d-1}$, so

$$\tilde{\mathcal{D}}_{d-1} \equiv \mathrm{Var}(m_{d-1} - x_d \mid \mathcal{F}_{d-1}) = \Omega_{d-1} + \sigma^2_{\varepsilon,d-1}/J.$$

**Parameterization.** To connect $\tilde{\mathcal{D}}_{d-1}$ to $\mathcal{D}_{d-1}$, we parameterize the split of observed disagreement by a constant share $\lambda \in [0,1]$:

$$B_{d-1} = \lambda\, \mathcal{D}_{d-1}, \qquad \sigma^2_{\varepsilon,d-1} = (1-\lambda)\mathcal{D}_{d-1},$$

and assume $\Omega_{d-1} = \omega B_{d-1}$ with $\omega > 0$ a scalar. Substituting into the expression for $\tilde{\mathcal{D}}_{d-1}$ delivers (6). Differentiation gives $\partial\tilde{\mathcal{D}}_{d-1}/\partial\mathcal{D}_{d-1} = \omega\lambda + (1-\lambda)/J > 0$.

### A.2 Day $d$: Structural and Measured Surprises

Define $\nu_d \equiv x_d - x_{d|d-1}$ (state innovation, variance $P_{d|d-1}$) and $\xi_{d-1} \equiv m_{d-1} - x_d$ (consensus error, variance $\tilde{\mathcal{D}}_{d-1}$). The Kalman update after observing the consensus is

$$x_{d|m} = x_{d|d-1} + K_{m,d-1}(m_{d-1} - x_{d|d-1}) = x_{d|d-1} + K_{m,d-1}(\nu_d + \xi_{d-1}),$$

where the second equality uses $m_{d-1} - x_{d|d-1} = \nu_d + \xi_{d-1}$. Substituting $a_d = x_d + \mu_{g_d} + u_d = x_{d|d-1} + \nu_d + \mu_{g_d} + u_d$ gives

$$\begin{aligned} s_d &= a_d - m_{d-1} = u_d - \xi_{d-1} + \mu_{g_d}, \\ \hat{s}_d &= a_d - x_{d|m} = (1 - K_{m,d-1})\nu_d + u_d - K_{m,d-1}\xi_{d-1} + \mu_{g_d}, \end{aligned}$$

and subtracting yields (8): $\hat{s}_d = s_d + (1 - K_{m,d-1})(m_{d-1} - x_{d|d-1})$.

The martingale property $E[\hat{s}_d \mid \mathcal{F}_{d-1}] = 0$ follows by writing $\hat{s}_d = (x_d - x_{d|m}) + u_d + \mu_{g_d}$: the first term has mean zero by optimality of $x_{d|m}$, the second by $E[u_d] = 0$, and the third by the normalization $p_{d-1}\mu_H + (1 - p_{d-1})\mu_L = 0$.

### A.3 Short Rate Uncertainty Decomposition

Under the anticipated utility approximation $\theta_{x,g_{d+k}} \approx \theta_{x,g_d}$ for $k \geq 0$,

$$r_{d+h} = \phi^h r_{d-1} + \theta_{x,g_d} X_h + U_h, \qquad X_h \equiv \sum_{j=0}^{h} \phi^{h-j} x_{d+j}, \quad U_h \equiv \sum_{j=0}^{h} \phi^{h-j} \eta_{d+j}.$$

The conditional independence of $\theta_{x,g_d}$ and $X_h$ given $\mathcal{F}_{d-1}$ decomposes the variance into

$$\mathrm{Var}(r_{d+h} \mid \mathcal{F}_{d-1}) = \mathrm{Var}(\theta_{x,g_d} X_h \mid \mathcal{F}_{d-1}) + \mathrm{Var}(U_h \mid \mathcal{F}_{d-1}).$$

Applying the product-variance formula (for independent $A, B$: $\mathrm{Var}(AB) = \mathrm{Var}(A)\,\mathrm{Var}(B) + \mathrm{Var}(A)(E[B])^2 + (E[A])^2\,\mathrm{Var}(B)$) to $\theta_{x,g_d} X_h$ and computing $\mu_{X,h}, \sigma^2_{X,h}, \bar{\theta}^{d-1}_x, \sigma^2_{\theta,d-1}$ as stated in Section 5.4 yields

$$\mathrm{Var}(\theta_{x,g_d} X_h \mid \mathcal{F}_{d-1}) = \sigma^2_{\theta,d-1}(\sigma^2_{X,h} + \mu^2_{X,h}) + (\bar{\theta}^{d-1}_x)^2 \sigma^2_{X,h},$$

and $\text{Var}(U_h \mid \mathcal{F}_{d-1}) = \sum_{j=0}^{h} \phi^{2(h-j)}\sigma_\eta^2$. Summing the two gives (10). The identity $\sigma^2_{\theta,d-1} = p_{d-1}(1-p_{d-1})(\Delta\theta_x)^2$ follows from writing $\theta_{x,g_d} = \theta_{x,L} + I_H\Delta\theta_x$ with $I_H \sim \text{Bernoulli}(p_{d-1})$.

### A.4 Release Informativeness and Posterior Beliefs

**Gaussian mixture and log odds.** Under (5), the regime conditional predictive densities of $a_d$ given $\mathcal{F}_{d|m} \equiv \mathcal{F}_{d-1} \cup \{m_{d-1}\}$ are Gaussian with means $\mu'_H = x_{d|m} + \Delta\mu/2$ and $\mu'_L = x_{d|m} - \Delta\mu/2$, common variance $\sigma_a^2 = P_{d|m} + \sigma_u^2$. Applying Bayes' rule to this Gaussian mixture and taking the log of the posterior odds,

$$\log\frac{f_H(a_d)}{f_L(a_d)} = \frac{\mu'_H - \mu'_L}{\sigma_a^2}\left(a_d - \tfrac{\mu'_H+\mu'_L}{2}\right) = \frac{\Delta\mu}{\sigma_a^2}(a_d - x_{d|m}) = \frac{\Delta\mu}{\sigma_a^2}\hat{s}_d.$$

Combining with the prior log odds gives (11).

**First order approximation of $\partial p_d/\partial a_d$.** Writing $p_d = z(\eta_0 + \kappa\hat{s}_d)$ with $z$ the logistic function, a Taylor expansion around $\hat{s}_d = 0$ gives $p_d \approx p_{d-1} + \kappa p_{d-1}(1-p_{d-1})\hat{s}_d$ and

$$p_d(1-p_d) \approx p_{d-1}(1-p_{d-1}) + \kappa\hat{s}_d p_{d-1}(1-p_{d-1})(1-2p_{d-1}) + O(\hat{s}_d^2).$$

Because $\partial\hat{s}_d/\partial a_d = 1$ (the posterior mean $x_{d|m}$ is predetermined on day $d-1$), $\partial p_d/\partial a_d = p_d(1-p_d)\kappa$. Taking expectations over a symmetric mean-zero $\hat{s}_d$ or evaluating at $p_{d-1} = 1/2$ kills the linear correction, leaving (12).

**Expected reduction in slope uncertainty.** Apply the law of total variance:

$$\underbrace{\text{Var}(\theta_{x,g_d} \mid \mathcal{F}_{d-1})}_{SU_{d-1}} = E[\text{Var}(\theta_{x,g_d} \mid \mathcal{F}_d) \mid \mathcal{F}_{d-1}] + \text{Var}[E(\theta_{x,g_d} \mid \mathcal{F}_d) \mid \mathcal{F}_{d-1}].$$

Using $\text{Var}(\theta_{x,g_d} \mid \mathcal{F}_d) = SU_d$ and $E[\theta_{x,g_d} \mid \mathcal{F}_d] = \theta_{x,L} + p_d\Delta\theta_x$, the second term equals $(\Delta\theta_x)^2\,\text{Var}(p_d \mid \mathcal{F}_{d-1})$. Rearranging gives (13).

### A.5 Yield-Response Coefficient (Linearization)

Using the anticipated-utility approximation,

$$E[r_{d+h} \mid \mathcal{F}_{d-1}] = \phi^h r_{d-1} + \sum_{j=0}^{h} \phi^{h-j} \bar{\theta}_x^{d-1} E[x_{d+j} \mid \mathcal{F}_{d-1}],$$
$$E[r_{d+h} \mid \mathcal{F}_{d}] = \phi^h r_{d-1} + \sum_{j=0}^{h} \phi^{h-j} \bar{\theta}_x^{d} E[x_{d+j} \mid \mathcal{F}_{d}].$$

The difference is nonlinear in $\hat{s}_d$ because both $\bar{\theta}_x^d$ and $E[x_{d+j} \mid \mathcal{F}_d]$ depend on $\hat{s}_d$. Linearize around $\hat{s}_d = 0$, using $E_d[x_{d+j} \mid \hat{s}_d = 0] = E_{d-1}[x_{d+j}]$ and $\bar{\theta}_x^d(0) = \bar{\theta}_x^{d-1}$:

$$\bar{\theta}_x^d(\hat{s}_d)\, E_d[x_{d+j} \mid \hat{s}_d] \approx \bar{\theta}_x^{d-1}\, E_{d-1}[x_{d+j}] + \bar{\theta}_x^{d-1}\, \rho^j K_{y,d}\, \hat{s}_d + \Delta\theta_x \frac{\partial p_d}{\partial a_d}\, E_{d-1}[x_{d+j}]\, \hat{s}_d.$$

Substituting and differentiating yields

$$\beta(\hat{s}_d) = G_h(\phi, \rho) \bar{\theta}_x^{d-1} K_{y,d} + \Delta\theta_x \frac{\partial p_d}{\partial a_d}\, \mu_{X,h}.$$

Replacing $\partial p_d / \partial a_d$ by its approximation (12) and using $SU_{d-1} = p_{d-1}(1 - p_{d-1})(\Delta\theta_x)^2$ gives (14).

### A.6 Attenuation Factor

The regime mean $\mu_{g_d}$ shifts $s_d$ and $\hat{s}_d$ by the same amount and is orthogonal to $\nu_d, u_d, \xi_{d-1}$, so it drops out of the covariance. Using the expressions for $s_d$ and $\hat{s}_d$ from Appendix A.2 and the orthogonality of $\nu_d, u_d, \xi_{d-1}$,

$$\begin{aligned} \operatorname{cov}(s_d, \hat{s}_d) &= \operatorname{cov}\big((1 - K_{m,d-1})\nu_d + u_d - K_{m,d-1}\xi_{d-1},\ u_d - \xi_{d-1}\big) \\ &= \operatorname{Var}(u_d) + K_{m,d-1} \operatorname{Var}(\xi_{d-1}) = \sigma_u^2 + K_{m,d-1}\tilde{\mathcal{D}}_{d-1}. \end{aligned}$$

Since $\operatorname{var}(s_d) = \sigma_u^2 + \tilde{\mathcal{D}}_{d-1}$, we obtain (16).

### A.7 Analytical Results: Derivations

**$\beta(\hat{s}_d)$ as an affine function of $SRU_{d-1,h}$.** From (10),

$$\sigma^2_{\theta,d-1} = \frac{SRU_{d-1,h} - (\bar{\theta}_x^{d-1})^2 \sigma^2_{X,h} - B_h(\phi, \sigma_\eta^2)}{\sigma^2_{X,h} + \mu^2_{X,h}},$$

where $B_h(\phi, \sigma_\eta^2) = \sum_{j=0}^{h} \phi^{2(h-j)} \sigma_\eta^2$. Substituting into (14) and using $\sigma_{\theta,d-1}^2/\Delta\theta_x = SU_{d-1}/\Delta\theta_x$ delivers

$$\beta(\hat{s}_d) = G_h(\phi,\rho)\bar{\theta}_x^{d-1} K_{y,d} - \frac{\Delta\mu}{\sigma_a^2\,\Delta\theta_x}\mu_{X,h}\left[\frac{(\bar{\theta}_x^{d-1})^2\sigma_{X,h}^2 + B_h(\phi,\sigma_\eta^2)}{\sigma_{X,h}^2 + \mu_{X,h}^2}\right] + \frac{\Delta\mu}{\sigma_a^2\,\Delta\theta_x}\frac{\mu_{X,h}}{\sigma_{X,h}^2 + \mu_{X,h}^2}\, SRU_{d-1,h}.$$

The first two terms define the intercept $C_{d,h}(\tilde{\mathcal{D}}_{d-1})$; the last is $\Lambda_{d,h}\, SRU_{d-1,h}$ with $\Lambda_{d,h}$ as in (18).

**Disagreement effect.** Holding $SRU_{d-1,h}$ fixed, (19) implies

$$\left.\frac{\partial \beta_h(s_d)}{\partial \mathcal{D}_{d-1}}\right|_{SRU} = \frac{\partial \tilde{\mathcal{D}}_{d-1}}{\partial \mathcal{D}_{d-1}}\left[\mathcal{A}_d'(\tilde{\mathcal{D}}_{d-1})\beta_h(\hat{s}_d) + \mathcal{A}_d(\tilde{\mathcal{D}}_{d-1})\left.\frac{\partial \beta_h(\hat{s}_d)}{\partial \tilde{\mathcal{D}}_{d-1}}\right|_{SRU}\right].$$

Because $\partial\tilde{\mathcal{D}}_{d-1}/\partial\mathcal{D}_{d-1} > 0$, the sign is the sign of the bracket. The first bracket term is negative ($\mathcal{A}_d' < 0$: attenuation); the second is positive ($K_{y,d}' > 0$: a noisier consensus raises residual state uncertainty, increasing the informativeness of the release). Ignoring the dependence of $\Lambda_{d,h}$ on $\tilde{\mathcal{D}}_{d-1}$, the structural amplification derivative simplifies to $G_h(\phi,\rho)\bar{\theta}_x^{d-1}K_{y,d}'(\tilde{\mathcal{D}}_{d-1})$, giving (26) below:

$$\left.\frac{\partial \beta_h(s_d)}{\partial \mathcal{D}_{d-1}}\right|_{SRU} \approx \frac{\partial \tilde{\mathcal{D}}_{d-1}}{\partial \mathcal{D}_{d-1}}\left[\mathcal{A}_d'(\tilde{\mathcal{D}}_{d-1})\,\beta_h(\hat{s}_d) + \mathcal{A}_d(\tilde{\mathcal{D}}_{d-1})\,G_h(\phi,\rho)\,\bar{\theta}_x^{d-1}\,K_{y,d}'(\tilde{\mathcal{D}}_{d-1})\right]. \tag{26}$$

### A.8 Proof of Proposition 1 (Closed Form Threshold)

Write $P \equiv P_{d|d-1}$, $\tilde{D} \equiv \tilde{\mathcal{D}}_{d-1}$, $\sigma^2 \equiv \sigma_u^2$. From the definitions,

$$\begin{aligned}
K_{m,d-1} &= P/(P+\tilde{D}), \qquad P_{d|m} = (1-K_{m,d-1})P = P\tilde{D}/(P+\tilde{D}),\\
K_{y,d} &= P_{d|m}/(P_{d|m}+\sigma^2) = P\tilde{D}/[P\tilde{D} + \sigma^2(P+\tilde{D})],\\
\mathcal{A}_d &= \left[\sigma^2(P+\tilde{D}) + P\tilde{D}\right] / \left[(\sigma^2+\tilde{D})(P+\tilde{D})\right].
\end{aligned}$$

Multiplying $\mathcal{A}_d$ by $K_{y,d}$, the common factor $\sigma^2(P+\tilde{D}) + P\tilde{D} = P\tilde{D} + \sigma^2(P+\tilde{D})$ cancels, leaving

$$\mathcal{A}_d K_{y,d} = \frac{P\tilde{D}}{(\sigma^2+\tilde{D})(P+\tilde{D})} \equiv f(\tilde{D}).$$

Differentiating, $f'(\tilde{D}) = P(\sigma^2 P - \tilde{D}^2)/[(\sigma^2+\tilde{D})(P+\tilde{D})]^2$, so $f'(\tilde{D}) = 0$ at $\tilde{D}^* = \sigma_u\sqrt{P}$, with $f' > 0$ for $\tilde{D} < \tilde{D}^*$ and $f' < 0$ for $\tilde{D} > \tilde{D}^*$.

# Appendix B Yield Response Derivation

This appendix derives the yield response coefficient used in Section 6.1 and the simulation.

## B.1 Futures Loading

For a single future horizon $\tau$, the expected short rate on day $d$ conditional on $\mathcal{F}_d$ is:

$$E_d[r_{d+\tau}] = \phi^{\tau+1} r_{d-1} + \bar{\theta}_x^d \sum_{j=0}^{\tau} \phi^{\tau-j} \rho^j x_{d|d} + 0$$

where we use the anticipated utility assumption $E_d[\theta_{x,g_{d+k}}] = \bar{\theta}_x^d$ for all $k > 0$, and $E_d[x_{d+j}] = \rho^j x_{d|d}$. The futures loading on the filtered state is:

$$G_\tau(\phi, \rho) = \sum_{j=0}^{\tau} \phi^{\tau-j} \rho^j$$

When $\phi \neq \rho$, this admits the closed form:

$$G_\tau(\phi, \rho) = \frac{\rho^{\tau+1} - \phi^{\tau+1}}{\rho - \phi} \tag{27}$$

## B.2 Yield Loading

The $h$-maturity zero-coupon yield under risk-neutral pricing is:

$$y_d^{(h)} = \frac{1}{h} \sum_{\tau=1}^{h} E_d[r_{d+\tau}]$$

The change in the yield around the announcement is:

$$\Delta y_d^{(h)} = \frac{1}{h} \sum_{\tau=1}^{h} \left( E[r_{d+\tau} | \mathcal{F}_d] - E[r_{d+\tau} | \mathcal{F}_{d-1}] \right)$$

The $\phi^{\tau+1} r_{d-1}$ terms cancel between the pre- and post-announcement expectations, leaving:

$$\Delta y_d^{(h)} = \frac{1}{h} \sum_{\tau=1}^{h} G_\tau \left( \bar{\theta}_x^d x_{d|d} - \bar{\theta}_x^{d-1} x_{d|m} \right) = \mathcal{B}_h \left( \bar{\theta}_x^d x_{d|d} - \bar{\theta}_x^{d-1} x_{d|m} \right) \tag{28}$$

where the yield loading is:

$$\mathcal{B}_h(\phi, \rho) = \frac{1}{h} \sum_{\tau=1}^{h} G_\tau(\phi, \rho)$$

The factorization in (28) follows because the bracket $\bar{\theta}_x^d x_{d|d} - \bar{\theta}_x^{d-1} x_{d|m}$ does not depend on $\tau$.

### B.3 Yield Response Coefficient

Linearizing the yield change around $\hat{s}_d = 0$ (as in the main text for futures) and using $x_{d|d} = x_{d|m} + K_{y,d}\hat{s}_d$, $\bar{\theta}_x^d(\hat{s}_d) \approx \bar{\theta}_x^{d-1} + \Delta\theta_x \frac{\partial p_d}{\partial \hat{s}_d}\hat{s}_d$:

$$\begin{aligned}\left.\frac{\partial \Delta y_d^{(h)}}{\partial \hat{s}_d}\right|_{\hat{s}_d=0} &= \mathcal{B}_h \left[\bar{\theta}_x^{d-1} K_{y,d} + \Delta\theta_x \left.\frac{\partial p_d}{\partial \hat{s}_d}\right|_{\hat{s}_d=0} x_{d|m}\right] \\ &= \underbrace{\mathcal{B}_h\, \bar{\theta}_x^{d-1}\, K_{y,d}}_{\text{State learning}} + \underbrace{\Delta\theta_x\, p_{d-1}(1-p_{d-1})\frac{\Delta\mu}{\sigma_a^2}\, \mathcal{B}_h\, x_{d|m}}_{\text{Slope learning}}\end{aligned}$$

This is equation (25) in the main text. The structure is identical to the futures-rate coefficient, with $\mathcal{B}_h$ replacing $G_h$ throughout, and $\mu_{X,h}^{\text{yield}} = \mathcal{B}_h \cdot x_{d|m}$.

### B.4 Yield Variance Terms and Short Rate Uncertainty

For the short-rate uncertainty measure adapted to yields, we need the variance of $\Delta y_d^{(h)}$ conditional on $\mathcal{F}_{d-1}$. Each future state $x_{d+j}$ enters the yield with weight:

$$w_j = \frac{1}{h}\sum_{\tau=j}^{h} \phi^{\tau-j} = \frac{1}{h}\cdot\frac{1-\phi^{h-j+1}}{1-\phi}, \quad j = 0, 1, \ldots, h$$

This is the yield weight on $x_{d+j}$, obtained by summing the contribution of $x_{d+j}$ to $r_{d+\tau}$ across all maturities $\tau \geq j$ and dividing by $h$. Using these weights, the yield analogues of the variance components are:

$$\sigma_{X,h}^{2,\text{yield}} = \sum_{j=0}^{h} w_j^2\, P_{d|d-1} \tag{29}$$

$$\mu_{X,h}^{\text{yield}} = \sum_{j=0}^{h} w_j \rho^j\, x_{d|m} = \mathcal{B}_h \cdot x_{d|m} \tag{30}$$

$$V_{U,h}^{\text{yield}} = \sum_{j=0}^{h} w_j^2\, \sigma_\eta^2 \tag{31}$$

and the yield-based short-rate uncertainty is:

$$SRU_{d-1,h}^{\text{yield}} = \sigma_{\theta,d-1}^2 \left(\sigma_{X,h}^{2,\text{yield}} + (\mu_{X,h}^{\text{yield}})^2\right) + (\bar{\theta}_x^{d-1})^2\, \sigma_{X,h}^{2,\text{yield}} + V_{U,h}^{\text{yield}} \tag{32}$$

The verification of (30) is provided below. Using $E_{d-1}[x_{d+j}] = \rho^j x_{d|m}$:

$$\mu_{X,h}^{\text{yield}} = \sum_{j=0}^{h} w_j \, \rho^j \, x_{d|m} = x_{d|m} \sum_{j=0}^{h} \frac{1}{h} \left( \sum_{\tau=j}^{h} \phi^{\tau-j} \right) \rho^j = \frac{x_{d|m}}{h} \sum_{j=0}^{h} \sum_{\tau=j}^{h} \phi^{\tau-j} \rho^j$$

Switching the order of summation ($j$ runs from 0 to $\tau$ for each $\tau$):

$$= \frac{x_{d|m}}{h} \sum_{\tau=1}^{h} \sum_{j=0}^{\tau} \phi^{\tau-j} \rho^j = \frac{x_{d|m}}{h} \sum_{\tau=1}^{h} G_\tau = \mathcal{B}_h \cdot x_{d|m}$$

# Appendix C Full Regression Tables

Table 7: Pre-2020 (1998–February 2020): Full regression results

| | 2-Year | 5-Year | 10-Year |
|---|---|---|---|
| *Surprise main effects* | | | |
| Durable | 0.00918*** | 0.0100*** | 0.00747*** |
| | (0.0014) | (0.0016) | (0.0013) |
| GDP (Advance) | 0.0102*** | 0.0141*** | 0.0108*** |
| | (0.0028) | (0.0036) | (0.0029) |
| Core CPI | 0.0129*** | 0.0172*** | 0.0140*** |
| | (0.0018) | (0.0022) | (0.0018) |
| Hourly Earn. | 0.0279*** | 0.0386*** | 0.0310*** |
| | (0.0049) | (0.0063) | (0.0051) |
| Retail ex. auto | 0.0160*** | 0.0190*** | 0.0150*** |
| | (0.0042) | (0.0046) | (0.0036) |
| Unemp. | -0.0338*** | -0.0386*** | -0.0275*** |
| | (0.0069) | (0.0079) | (0.0062) |
| Init. Claims | -0.0291*** | -0.0335*** | -0.0276*** |
| | (0.0027) | (0.0031) | (0.0025) |
| CPI | 0.000539 | 0.00292 | 0.00297* |
| | (0.0017) | (0.0020) | (0.0016) |
| Nonfarm | 0.246*** | 0.290*** | 0.219*** |
| | (0.0231) | (0.0277) | (0.0228) |
| Retail | 0.0101** | 0.0135*** | 0.0107*** |
| | (0.0040) | (0.0044) | (0.0036) |
| *Disagreement and uncertainty levels* | | | |
| $disp^{Retail}$ | -0.00912** | -0.0102** | -0.00804** |
| | (0.0040) | (0.0047) | (0.0040) |
| $disp^{Init.Claims}$ | 0.000381 | 0.000207 | 0.000468 |
| | (0.0010) | (0.0012) | (0.0010) |
| $disp^{CPI}$ | -0.000915 | -0.000663 | -0.000410 |
| | (0.0016) | (0.0020) | (0.0017) |
| $disp^{Nonfarm}$ | -0.0353*** | -0.0426*** | -0.0373*** |
| | (0.0068) | (0.0102) | (0.0082) |
| $disp^{durable}$ | 0.00212 | 0.00114 | 0.000801 |
| | (0.0020) | (0.0024) | (0.0020) |
| $disp^{GDP}$ | -0.0103 | -0.0123 | -0.00986 |
| | (0.0077) | (0.0102) | (0.0085) |
| $SRU$ | -0.000199 | -0.000757 | -0.000326 |
| | (0.0009) | (0.0011) | (0.0009) |
| *Interaction terms* | | | |
| Init. Claims × $disp^{Init.Claims}$ | 0.00431 | 0.00752** | 0.00717*** |
| | (0.0030) | (0.0033) | (0.0027) |
| Init. Claims × $SRU$ | -0.0161*** | -0.0136*** | -0.00832*** |
| | (0.0030) | (0.0036) | (0.0029) |
| CPI × $disp^{CPI}$ | -0.00226** | -0.00345** | -0.00279** |
| | (0.0010) | (0.0014) | (0.0011) |
| CPI × $SRU$ | -0.000246 | -0.00169 | -0.000599 |
| | (0.0017) | (0.0021) | (0.0017) |
| Nonfarm × $disp^{Nonfarm}$ | -0.176*** | -0.260*** | -0.220*** |
| | (0.0594) | (0.0808) | (0.0627) |
| Nonfarm × $SRU$ | 0.0932*** | 0.0710*** | 0.0352* |
| | (0.0209) | (0.0262) | (0.0195) |
| Durable × $disp^{durable}$ | -0.00483** | -0.00415* | -0.00411** |
| | (0.0023) | (0.0023) | (0.0019) |
| Durable × $SRU$ | 0.00600*** | 0.00524*** | 0.00284* |
| | (0.0017) | (0.0018) | (0.0015) |
| Retail × $disp^{Retail}$ | -0.00318 | -0.00315 | -0.00424 |
| | (0.0049) | (0.0052) | (0.0044) |
| Retail × $SRU$ | 0.0122*** | 0.00968** | 0.00749** |
| | (0.0037) | (0.0039) | (0.0032) |
| GDP × $disp^{GDP}$ | -0.0247*** | -0.0331*** | -0.0266*** |
| | (0.0093) | (0.0116) | (0.0089) |
| GDP × $SRU$ | 0.00707** | 0.00667* | 0.00406 |
| | (0.0030) | (0.0038) | (0.0031) |

Continued on next page.

Table 8: Pre-2020 (1998–February 2020): Full regression results (continued)

| | 2-Year | 5-Year | 10-Year |
|---|---|---|---|
| *Quadratic terms* | | | |
| Durable$^2$ | -0.00220** | -0.00211*** | -0.00163** |
| | (0.0009) | (0.0008) | (0.0007) |
| GDP$^2$ | 0.00196 | 0.00292 | 0.00233 |
| | (0.0020) | (0.0026) | (0.0021) |
| Init. Claims$^2$ | -0.00691 | -0.00568 | -0.00446 |
| | (0.0074) | (0.0088) | (0.0071) |
| CPI$^2$ | -0.00109 | -0.000339 | -0.000256 |
| | (0.0009) | (0.0013) | (0.0010) |
| Nonfarm$^2$ | 0.202*** | 0.202*** | 0.136** |
| | (0.0653) | (0.0780) | (0.0639) |
| Retail$^2$ | -0.000139 | -0.000587 | -0.0000264 |
| | (0.0020) | (0.0024) | (0.0020) |
| $(disp^{Retail})^2$ | 0.000174 | -0.000180 | 0.000452 |
| | (0.0068) | (0.0068) | (0.0058) |
| $(disp^{CPI})^2$ | -0.000469 | -0.000791 | -0.000667 |
| | (0.0006) | (0.0009) | (0.0007) |
| $(disp^{Nonfarm})^2$ | 0.0129 | 0.0144 | 0.00964 |
| | (0.0104) | (0.0174) | (0.0142) |
| $(disp^{Durable})^2$ | 0.00386** | 0.00333** | 0.00308** |
| | (0.0017) | (0.0016) | (0.0013) |
| $(disp^{GDP})^2$ | -0.0117 | -0.0133 | -0.0103 |
| | (0.0085) | (0.0111) | (0.0092) |
| $SRU^2$ | -0.000160 | 0.000507 | 0.000791 |
| | (0.0007) | (0.0008) | (0.0007) |
| *Controls* | | | |
| VIX | 0.000937 | 0.000751 | 0.000878 |
| | (0.0008) | (0.0010) | (0.0008) |
| MOVE | 0.000133 | 0.000708 | 0.000299 |
| | (0.0013) | (0.0016) | (0.0013) |
| EPU | 0.000401 | 0.000420 | 0.000428 |
| | (0.0006) | (0.0007) | (0.0006) |
| JLN | 0.00216** | 0.00281*** | 0.00206** |
| | (0.0009) | (0.0010) | (0.0008) |
| ZLB | -0.00293*** | -0.00325** | -0.00205* |
| | (0.0010) | (0.0013) | (0.0011) |
| Constant | 0.00274*** | 0.00186* | 0.000938 |
| | (0.0009) | (0.0010) | (0.0008) |
| Observations | 2,383 | 2,516 | 2,517 |
| R-squared | 0.425 | 0.406 | 0.380 |

* $p < 0.10$, ** $p < 0.05$, *** $p < 0.01$. Standard errors in parentheses.

Table 9: Post-COVID (July 2020–2024): Full regression results

| | 2-Year | 5-Year | 10-Year |
|---|---|---|---|
| *Surprise main effects* | | | |
| Durable | -0.0106 | -0.00625 | -0.00101 |
| | (0.0105) | (0.0074) | (0.0047) |
| GDP (Advance) | -0.00995 | -0.0120* | -0.0115*** |
| | (0.0142) | (0.0067) | (0.0044) |
| Core CPI | 0.0272*** | 0.0344*** | 0.0250*** |
| | (0.0094) | (0.0094) | (0.0069) |
| Hourly Earn. | 0.0490*** | 0.0450*** | 0.0316*** |
| | (0.0153) | (0.0152) | (0.0117) |
| Retail ex. auto | 0.00413 | 0.00579 | 0.00430 |
| | (0.0076) | (0.0077) | (0.0058) |
| Unemp. | -0.0272** | -0.0295** | -0.0205** |
| | (0.0116) | (0.0121) | (0.0096) |
| Init. Claims | -0.0308 | -0.0414*** | -0.0305*** |
| | (0.0316) | (0.0115) | (0.0075) |
| CPI | 0.0216 | 0.0162 | 0.0104 |
| | (0.0131) | (0.0122) | (0.0088) |
| Nonfarm | 0.191*** | 0.205*** | 0.150*** |
| | (0.0446) | (0.0466) | (0.0388) |
| Retail | -0.0109 | 0.00629 | 0.00595 |
| | (0.0269) | (0.0153) | (0.0109) |
| *Disagreement and uncertainty levels* | | | |
| $disp^{Retail}$ | 0.0171 | -0.0112 | -0.00492 |
| | (0.0424) | (0.0138) | (0.0103) |
| $disp^{Init.Claims}$ | -0.00188 | -0.000167 | 0.000497 |
| | (0.0017) | (0.0011) | (0.0008) |
| $disp^{CPI}$ | 0.000657 | 0.00750 | 0.0101 |
| | (0.0095) | (0.0095) | (0.0069) |
| $disp^{Nonfarm}$ | 0.00222 | 0.00473 | 0.00525 |
| | (0.0056) | (0.0058) | (0.0044) |
| $disp^{Durable}$ | 0.00211 | 0.00157 | 0.00172 |
| | (0.0093) | (0.0046) | (0.0036) |
| $disp^{GDP}$ | 0.0243 | -0.00474 | -0.00332 |
| | (0.0319) | (0.0087) | (0.0041) |
| $SRU$ | -0.00376 | 0.00129 | 0.000167 |
| | (0.0085) | (0.0054) | (0.0037) |
| *Interaction terms* | | | |
| Init.Claims × $disp^{Init.Claims}$ | 0.000619 | 0.000817 | 0.000980** |
| | (0.0009) | (0.0006) | (0.0004) |
| Init.Clams × $SRU$ | -0.0139 | -0.0201*** | -0.0136*** |
| | (0.0191) | (0.0067) | (0.0043) |
| CPI × $disp^{CPI}$ | -0.0335** | -0.0358** | -0.0312*** |
| | (0.0162) | (0.0152) | (0.0107) |
| CPI × $SRU$ | 0.0275*** | 0.0306*** | 0.0216*** |
| | (0.0062) | (0.0066) | (0.0053) |
| Nonfarm × $disp^{Nonfarm}$ | -0.0344* | -0.0258 | -0.0160 |
| | (0.0198) | (0.0207) | (0.0171) |
| Nonfarm × $SRU$ | 0.0166 | 0.0244 | 0.0208 |
| | (0.0247) | (0.0251) | (0.0206) |
| Durable × $disp^{Durable}$ | 0.00541 | -0.0000503 | -0.00735 |
| | (0.0153) | (0.0116) | (0.0077) |
| Durable × $SRU$ | 0.00666 | 0.000328 | -0.000891 |
| | (0.0058) | (0.0037) | (0.0028) |
| Retail × $disp^{Retail}$ | -0.000675 | -0.0116** | -0.00951** |
| | (0.0138) | (0.0053) | (0.0038) |
| Retail × $SRU$ | -0.00891 | -0.00279 | -0.00201 |
| | (0.0085) | (0.0053) | (0.0038) |
| GDP × $disp^{GDP}$ | 0.0209 | 0.0143 | 0.0130* |
| | (0.0138) | (0.0102) | (0.0072) |
| GDP × $SRU$ | 0.00385 | 0.00510 | 0.00484 |
| | (0.0046) | (0.0049) | (0.0037) |

Continued on next page.

Table 10: Post-COVID (July 2020–2024): Full regression results (continued)

| | 2-Year | 5-Year | 10-Year |
|---|---|---|---|
| *Quadratic terms* | | | |
| Durable$^2$ | 0.00415 | 0.00173 | 0.00239 |
| | (0.0028) | (0.0028) | (0.0017) |
| GDP (Advance)$^2$ | -0.000114 | -0.000302 | -0.000901 |
| | (0.0034) | (0.0017) | (0.0013) |
| Init. Claims $^2$ | 0.00200 | -0.000483 | -0.000122 |
| | (0.0024) | (0.0014) | (0.0010) |
| CPI $^2$ | -0.00290 | -0.00129 | -0.000967 |
| | (0.0036) | (0.0039) | (0.0031) |
| Nonfarm $^2$ | -0.00539 | 0.00584 | 0.00439 |
| | (0.0432) | (0.0479) | (0.0392) |
| Retail $^2$ | -0.00232* | -0.00117 | -0.000887 |
| | (0.0014) | (0.0009) | (0.0007) |
| $(disp^{Retail})^2$ | -0.00309 | 0.0116* | 0.00803 |
| | (0.0207) | (0.0069) | (0.0050) |
| $(disp^{CPI})^2$ | 0.00436 | 0.00576 | 0.00756 |
| | (0.0119) | (0.0113) | (0.0079) |
| $(disp^{Nonfarm})^2$ | -0.00189*** | -0.00199*** | -0.00152*** |
| | (0.0007) | (0.0007) | (0.0005) |
| $(disp^{Durable})^2$ | 0.0000187 | -0.000186 | 0.000803 |
| | (0.0050) | (0.0031) | (0.0024) |
| $(disp^{GDP})^2$ | -0.00919 | -0.00224 | -0.00212 |
| | (0.0075) | (0.0027) | (0.0016) |
| $SRU^2$ | 0.00158 | 0.000667 | 0.000145 |
| | (0.0021) | (0.0014) | (0.0010) |
| *Controls* | | | |
| VIX | 0.00696 | 0.00281 | 0.00374 |
| | (0.0062) | (0.0036) | (0.0026) |
| MOVE | 0.00645 | -0.00222 | -0.00183 |
| | (0.0139) | (0.0080) | (0.0055) |
| EPU | 0.00160 | 0.00112 | 0.000428 |
| | (0.0040) | (0.0025) | (0.0018) |
| JLN | -0.000399 | -0.00439 | -0.00590 |
| | (0.0066) | (0.0049) | (0.0036) |
| ZLB | 0.00541 | 0.00275 | -0.000563 |
| | (0.0098) | (0.0078) | (0.0057) |
| Constant | -0.00815 | 0.00205 | 0.00699 |
| | (0.0103) | (0.0064) | (0.0044) |
| Observations | 375 | 375 | 375 |
| R-squared | 0.247 | 0.546 | 0.552 |

* $p < 0.10$, ** $p < 0.05$, *** $p < 0.01$. Standard errors in parentheses.